National Aeronautics and
Space Administration
John H. Glenn Research Center
Lewis Field
Plum Brook Station
Sandusky, OH 44870

January 30, 2008

Reply to Attn of: QD

U.S. Nuclear Regulatory Commission
Attn: Document Control Desk
Washington, D.C. 20555

Subject: Plum Brook Reactor Facility, Licenses Nos. TR-3, Docket No. 50-30 and R-93, Docket No, 50-185, Technical Basis for Use of Paired Measurements in Assessing Gross Beta DCGLs During Structure Surface Surveys

During an inspection performed at the site from November 26 through November 28, 2008, and in a telephone conference call on December 6, 2007, the NRC Staff raised questions on the design basis for probe shields used in the performance of fixed point surveys of building surface structures.

These surveys are used in assessing the gross beta DCGL for building structure surfaces. Shielded and unshielded surface readings are compared to assess the pure beta component of the residual activity. Questions were raised by the staff on how we assure that the higher energy contribution from the Sr/Y-90 beta is shielded out in the unshielded readings. The attached Technical Basis Document provides documented calculations and design analyses that support the shielded design used in the performance of these surveys.

Should you have any questions or need additional information, please contact me a NASA Plum Brook Station, 6100 Columbus Avenue, Sandusky, Ohio 44870, or by telephone at (419) 621-3277.

Sincerely,

Keith M. Peecook
Program Manager

Enclosure
1. Technical Basis Document PBRF-TBD-07-006, "Shield Analyses for the Ludlum 44-116 Probe", Revision 0, dated January 30, 2008

A020
FSME

cc:
USNRC/C. J. Glenn (FSME)
USNRC/J. Webb (FSME) – CDROM copy
USNRC/W. G. Snell RIII/DNMS/DB – CDROM copy
USNRC/P. J. Lee RIII/DNMS/DB – CDROM copy
ODH/M. J. Rubadue – CDROM copy

Plum Brook Reactor Facility

Technical Basis Document

Beta Shield Analysis for the Ludlum Model 44-116 Probe

PBRF-TBD-07-006
Revision No. 0

Prepared By:	[signature]	Date:	1/30/08
Independent Technical Review:	[signature]	Date:	1/30/08
Other Review:	N/A	Date:	
Other Review:	N/A	Date:	
Cognizant Manager Approval:	W. Stoner / [signature]	Date:	1/30/08
RSO Approval:	W. Stoner / [signature]	Date:	1/30/08

Form
AD-04/02
Rev. 0

NASA PBRF DECOMMISSIONING PROJECT CHANGE/CANCELLATION RECORD		
DOCUMENT TITLE: Beta Shield Analysis for the Ludlum Model 44-116 Probe	**DOCUMENT NO: PBRF-TBD-07-006**	**REVISION NO: 0**
<u>Revision 0</u>: Initial issue of Document		

LIST OF EFFECTIVE PAGES

DOCUMENT NO: **PBRF-TBD-07-006** **REVISION NO.:** **0**

Page No.	Revision Level	Page No.	Revision Level	Page No.	Revision Level
Cover Page	0				
Change/Cancellation Record	0				
LOEP	0				
TOC , Lists of Figures and Tables & Glossary	0				
TBD-07-006 Report Pages 1 thru 18	0				
Appendix A Page 19 thru 31	0				
Appendix B Page 32 thru 34	0				
Appendix C Page 35 thru 41	0				
Appendix D Page 42 thru 45	0				

Form
AD-01/ 5
Rev 2

TABLE OF CONTENTS

APPENDICES

LIST OF FIGURES

LIST OF TABLES

GLOSSARY

absorber – the material placed between source and detector so as to reduce the number of beta particles reaching the detector

density – an object's mass divided by its volume, generally has units of kg/m^3 or mg/cm^3

density thickness – an object's density multiplied by its thickness, has units of mg/cm^2 – using these units makes it possible to express the amount of material needed to stop beta particles of a specific energy independent of the absorber material

dpm – disintegrations per minute

dps – disintegrations per second

range – the absorber thickness (in centimeters) that reduces the beta particle count to background - the range of charged particles of a specific energy is unique in a specific absorber material; however, if units of mg/cm^2 are used, then specifying the absorber material is not needed (see density thickness)

1.0 PURPOSE

The purpose of this Technical Basis Document is to determine the "range" of shielding material needed to completely block all Sr/Y-90 betas from their detection by a Ludlum Model 44-116 probe. This is to ensure that unshielded readings (beta plus gamma) minus shielded readings (gamma only) provide the true beta-only response. In similar fashion to a Feather Analysis, various shields will be placed in between a Sr/Y-90 source and a Ludlum Model 44-116 probe (thin plastic scintillator), while maintaining the overall distance (air plus shields) constant, to determine the detector's response.

2.0 BACKGROUND

During its most recent on-site visit, the Nuclear Regulatory Commission expressed doubt as to the ability of the Ludlum Model 44-116 shield, currently used by the Final Status Survey (FSS) team, to keep all beta particles from reaching the thin plastic scintillation material in the probe. FSS collects unshielded (beta plus gamma) and shielded (gamma only) measurements and subtracts the two to obtain beta measurements. These beta measurement are compared the Derived Concentration Guideline Level (DCGL) in order to determine whether or not an area may be released for the purpose of license termination.

Step 4.3.3.5 of Plum Brook Reactor Facility (PBRF) procedure CS-01, Survey Methodology to Support PBRF License Termination requires that shielded readings be taken by completely covering the detector window with approximately 3/8" (900 mg/cm^2) of Plexiglas, Lucite, or other equivalent shield material.

There are two shields (thin and thick) used to conduct final status surveys which are in use presently. The thin shield [LMI 2007] is constructed of stainless steel with density of 7.9292 g/cm^3 and thickness of 0.018 inches. It is manufactured by Ludlum Measurements, Inc. of Sweetwater, Texas. Both the thick shield's construction material and manufacture are unknown. The material is assumed to be stainless steel as its estimated density (mass divided by its estimated volume) approximates that of iron. The thickness is estimated to be 0.034" by digital caliper taking multiple measurements around the edges of the shield. A quick calculation, multiplying the density by the shield thickness in inches, reveals the thin shield to be about 363 mg/cm^2 and the thick shield to be about 685 mg/cm^2.

2.1 Beta Emission

A beta particle is an ordinary electron that is ejected from the nucleus of an unstable radioactive atom. The beta particle is formed at the instant of emission by the transformation of a neutron into a proton and an electron. The existence of the neutrino was postulated because, contrary to the expectation of mono-energetic emission, beta particles were shown to occur in a continuous energy spectrum up to the maximum beta energy. The neutrino has no electrical charge and extremely small mass. As such, it carries away some energy and conserves momentum since, experimentally, it has been shown that the neutrino energy is equal to the difference between the kinetic energy of the accompanying beta particle and the maximum energy of the spectral distribution. Generally, the average beta energy is about 30%-40% of the maximum beta energy. Unless otherwise noted, when the energy of a beta emitter is given, it is the maximum energy [CEM 1983, pp. 63-65]. A typical beta energy spectrum [NSF 2004] is shown below.

Figure 2.1

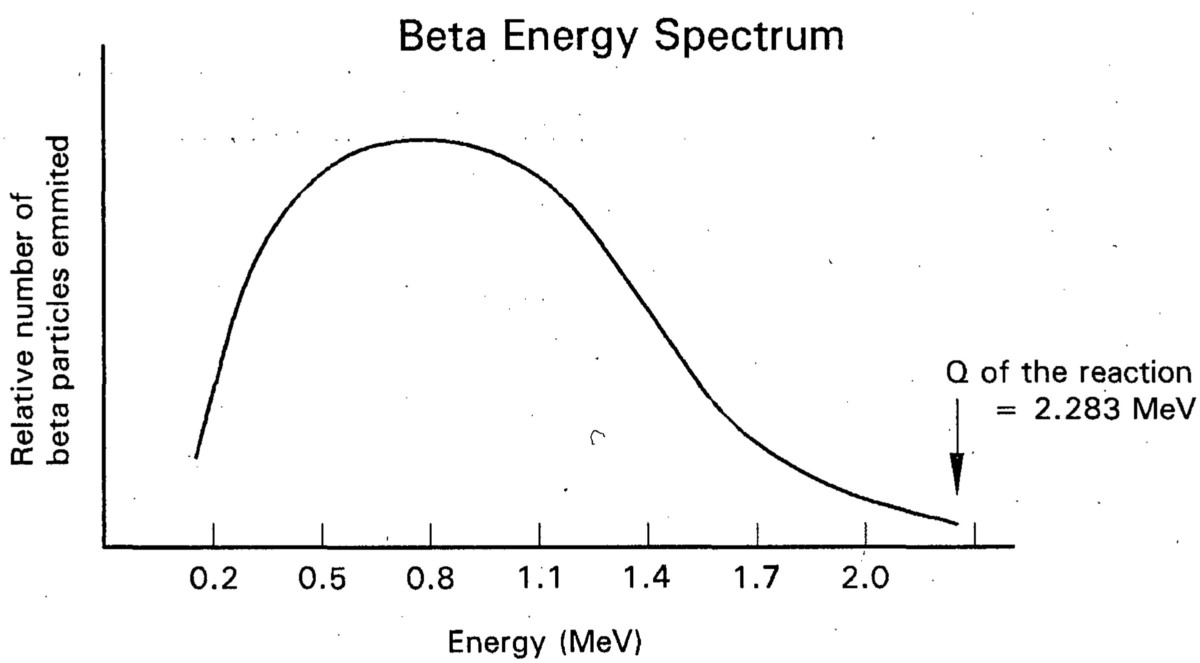

In Sr-90, beta emission [USDH 1970, p. 266] occurs according to the following equation

$$^{90}_{38}Sr \xrightarrow{T_{1/2}=28.6\,yr.} {}^{90}_{39}Y + {}^{0}_{-1}e + 0.546\,MeV + \upsilon. \qquad \textbf{(Eq. 2-1)}$$

where: ${}^{0}_{-1}e$ is the beta particle
υ is the anti-neutrino

This reaction occurs 100% of the time. The average beta energy is about 0.1958 MeV [HACK 2001].

Similarly, Y-90 emits a beta particle [USDH 1970, p. 268] according to the following equation

$$^{90}_{39}Y \xrightarrow{T_{1/2}=64.1\,hr.} {}^{90}_{40}Zr + {}^{0}_{-1}e + 2.2839\,MeV + \upsilon. \qquad \textbf{(Eq. 2-2)}$$

This reaction occurs almost 100% of the time. The average beta energy is about 0.9348 MeV [HACK 2001]. Zr-90 is stable. With a probability of 0.000115, Y-90 emits a 0.5232 MeV beta followed by a 1.7607 MeV photon. The average energy for this emission is 0.1865 keV [HACK 2001][USDH 1970].

2.2 Feather Analysis

Feather Analysis [EVAN 1955] is a technique for determining R_m (Feather's notation for maximum range) of beta particles by comparing the absorption curve whose end point is R_m to that of a well-established standard (Feather used RaE which is Bi-210). The two curves are normalized to the same initial value on a plot of logarithmic transmission versus absorber thickness (see Figure 2.2).

Figure 2.2
Log Transmitted Intensity versus Absorber Thickness

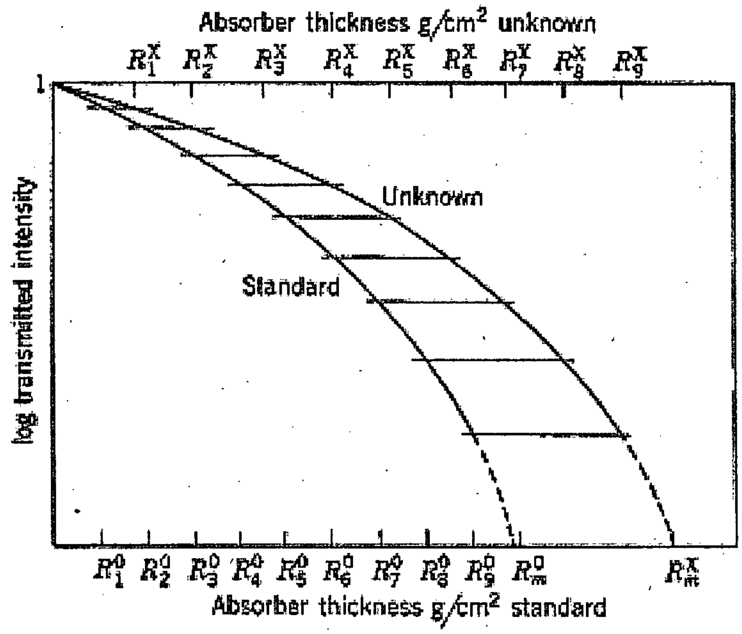

The range of the standard curve is now divided into N equal parts (Feather used N=10, as does Figure 2.2). These parts are designated R_n^0 and the end point which has been well established is marked R_m^0. The fractional transmission corresponding to these absorber thicknesses is marked on the standard curve. Points corresponding to the same relative transmission are now marked on the unknown curve. These are the intersections of horizontal lines and the unknown curve. The absorber thickness corresponding to these transmission values is now marked on the scale of absorber thickness for the unknown (upper abscissa) and is designated R_m^X. The maximum range R_m of the unknown is now the limiting value of $\left(\frac{N}{n}\right)R_m^X$ as $n \longrightarrow N$, in this case as $n \longrightarrow 10$. This maximum range can be obtained graphically by plotting $\left(\frac{N}{n}\right)R_m^X$ as a function of n, connecting the points by a smooth curve, and reading the value of R_m^X from the extrapolated intercept of the curve with the n = N axis, as shown in Figure 2-3 below.

Figure 2.3

Plot of $\left(\frac{N}{n}\right)R_m^X$ versus n

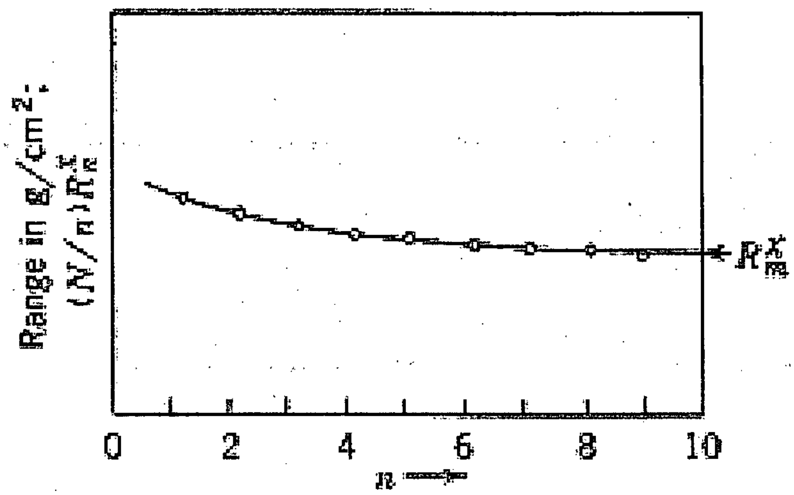

The PBRF does not possess a well-established standard; however, use of Feather's original work aids in developing a modified Feather Analysis (see Section 4.0) used in the completion of this Technical Basis Document.

Originally, Feather's Rule [USDH 1970, p. 92] for beta particle range (R) was

$$R = 542E - 133 \qquad (E > 0.6\ \text{MeV, R in mg/cm}^2). \qquad \textbf{(Eq. 2-3)}$$

The rule has been modified over the years and fit to the following formula which works over a broad range of energies. This Range-Energy [USDH 1970, p. 29] equation is

$$R = 412E^{1.265-0.0954\ln E} \qquad (\text{E in MeV, R in mg/cm}^2). \qquad \textbf{(Eq. 2-4)}$$

The ranges for the various Strontium and Yttrium beta particles, for both Feather's Rule and the Range-Energy equations, are shown in Table 2-1 below.

Table 2-1
Maximum Beta Energies and Ranges of Sr-90 and Y-90 Beta Particles

Radionuclide	Energy (MeV)	Probability	Feather's Rule Range (mg/cm^2)	Range-Energy Range (mg/cm^2)
Sr-90	0.5460	1.000000	*	185.0436
Y-90	0.5232	0.000115	*	174.4318
Y-90	2.2839	0.999890	1104.8738	1097.3973

* Feather's Rule is only defined for E > 0.6MeV

2.3 Strontium 90 Source

The Sr-90 provided to NASA Plum Brook for this analysis was provided by the NASA Glenn Research Center in Cleveland, Ohio. The source certification and photos of the source are shown in Appendix A of this document. From Section 2.1 above, one can see the half lives of the Sr-90 and Y-90 are 28.6 years and 64.1 hours, respectively. Because the half life of the parent is very much longer than that of the daughter, they are presumed to be in secular equilibrium.

3.0 REFERENCES

CEM 1983 — Cember, Herman. *Introduction to Health Physics*. 2nd Edition. Pergamon Press, New York, N.Y. 1983.

EVAN 1955 — Evans, Robley D. *The Atomic Nucleus*. McGraw-Hill Book Company, Inc. New York, N.Y. 1955.

HACK 2001 — Hacker, Charles. *Radiation Decay Version 3.6*. Griffith University – Gold Coast Campus, School of Engineering, Gold Coast, Australia. May, 2001.

JOHN 1964 — Johnson, N.L. and Fred Leone. *Statistics and Experimental Design*. John Wiley & Sons, Inc. New York, N.Y. 1964.

LMI 2006 — Ludlum Measurements, Inc. *2006 Product Catalog*. Ludlum Measurements, Inc. Sweetwater, Texas. October 27, 2006. (http://www.ludlums.com/product.htm)

LMI 2007 — Ludlum Measurements, Inc. *Facsimile of Model 43-89 Protective Cover*. Ludlum Measurements, Inc. Sweetwater, Texas. December , 2007.

NSF 2004 — National Science Foundation. *Research Experience for Undergraduates Program*. University of North Carolina at Pembroke. Pembroke, North Carolina. Summer, 2004. (http://www.uncp.edu/home/dooling/research/Maureen%20SERMACS%20poster.ppt#275,6,Yttrium-90 Beta Spectrum)

USDH 1970 United States Department of Health, Education, and Welfare. *Radiological Health Handbook.* 1970.

WIKI 2008 Wikipedia®, "*Density_of_air*", Wikimedia Foundation Inc. January 16, 2008. (http://en.wikipedia.org/wiki/Density_of_air)

4.0 DESCRIPTION OF EXPERIMENT

In this section, refer to Appendix A to view drawings and photographs of the source and source/probe setup. Also, refer to Appendix B for all data taken during the course of this experiment.

Section 2.0 describes how Feather's Analysis is used. Not mentioned in that section were particulars like:

A. a point source (Bi-210 in this case) was used as the reference standard,
B. aluminum absorbers (sometimes called calibrated absorbers) were used, and
C. a thin (mica), end window Geiger-Mueller detector was used in the analysis.

As mentioned in Section 2.0, this Technical Basis Document uses what will be described as a modified Feather Analysis. The following describes the main differences between the approach used in this Technical Basis Document and Feather's approach.

A. a disk source of Sr/Y-90 that is approximately 1 5/8" diameter,
B. absorbers, made on site, of 0.010 inch-thick aluminum sheet, and
C. use of a Ludlum Model 44-116, mylar-covered, large-area, plastic scintillation detector.

This technique can simply be described as placing a detector a fixed distance from a source and gradually inserting sheets of aluminum between the source and the detector and measuring the count rates. Data will be plotted on semi-logarithmic graph paper so that one can see the exponential reduction in the number of counts versus density thickness. The more sheets of aluminum placed between the source and detector, the less the count rate. When the count rate has decreased to background, the end point energy has been reached. At this point, one measures the thickness of aluminum and multiplies by the density of aluminum to obtain the range of the beta particle in the material.

4.1 Air Density

In order to account for the density thickness of the air gap between the source and probe, the air density must be known. On 12/18/07 the barometric pressure was 1018.2 mbars and the temperature in PBRF Trailer 11 was 60 degrees Fahrenheit owing to heater problems. The equation for dry air density [WIKI 2008] is shown below.

$$\rho_{air} = \frac{P_d}{R_d T} \qquad \textbf{(Eq. 4-1)}$$

where: $P_d \equiv$ atmospheric pressure in Pascals (1 mbar = 100 Pascals and 1 Pa = 1 N/m^2)
$R_d \equiv$ gas constant 287.05 J/kg-^{o}K (for dry air)
$T \equiv$ absolute temperature in degrees Kelvin
$\rho_{air} \equiv$ density of air in kg/ m^3 (or mg/cm^3)
$^0K \equiv 273.15 + \frac{5}{9}\left({}^0F - 32\right)$

The density of air on 12/18/07 was calculated to be

$$\rho_{air} = \frac{100\dfrac{Pa}{mbar}(1018.2mbar)}{\left[287.05\dfrac{J}{kg-{}^oK}\right]\left[273.15 + \dfrac{5}{9}(60-32)\right]{}^oK} = 1.229\frac{kg}{m^3} \qquad \textbf{(Eq. 4-2)}$$

4.2 Initial Setup

The probe is set up on four, one-inch-tall, wooden blocks. The total distance from the face of the mylar on the source to the face of the mylar over the plastic scintillator is 0.97875 inches (2.486025 cm) (see Appendix A, Scale Drawing of Setup).

Per Ludlum (LMI 2006), the probe mylar is 1.2 mg/cm^2. Per the source certificate, the mylar covering the source is 0.9 mg/cm^2. The total density thickness of mylar is 2.1 mg/cm^2 and the thickness of mylar is 0.000788 cm (2.1 mg/cm^2 divided by 2700 mg/cm^3 density).

The thickness of air is 2.486025 cm minus 0.000788 cm or 2.485247 cm.

Multiplying the density of air by the thickness of air gives the range in air.
(1.229 g/cm^3) x (2.485247 cm) = 3.053 mg/cm^2.

The total density thickness of air and mylar is 3.053 mg/cm^2 plus 2.1 mg/cm^2 or 5.153 mg/cm^2. The initial setup starts at 5.153 mg/cm^2 with no aluminum shields in place.

Each piece of aluminum is 0.010 inches thick (0.0254 cm). The density thickness of each piece of aluminum is calculated by multiplying 2700 mg/cm^3 by 0.0254 cm to obtain 68.58 mg/cm^2. Each 0.010 inch-thick slice of air is 1.229 mg/cm^3 times 0.0254 cm or 0.031 mg/cm^2. When calculating the overall density thickness, the density thickness of a slice of aluminum is added while the density thickness of an equivalent thickness of air is subtracted.

4.3 Measurements

An FSS Technician was assigned to take a single series of 10 one-minute measurements to establish the background count for the Ludlum Model 44-116 probe.

Following that, 21 series of 10 one-minute counts were taken with the Sr/Y-90 source in place. The series measurements were taken with a number of 0.010-inch-thick sheets of aluminum placed between the source and probe. A true Feather Analysis would have used a series of aluminum absorbers; however, absorbers were not available for this experiment, so thin aluminum sheets were used as a substitute. Absorbers, sometimes called calibrated absorbers, are single pieces of aluminum of various thicknesses milled to within thousandths of an inch over the surface so as to maintain continuity of the surface as well is thickness of the absorber,

Next, three series of 10 one-minute counts were taken on pieces of translucent plastic that were ordered previously from McMaster-Carr. One sheet was said to be ¼"-thick, the other ½"-thick, and, by default, the sum of the two was ¾"-thick. Using a caliper, it was determined that the ¼" piece was actually 0.255 inches thick, the ½" piece was 0.49 inches thick, and the combination of the two was 0.745" thick. Each piece was within the thickness specifications offered by McMaster-Carr; however, upon contacting them, no person at McMaster-Carr could find the density of the material but the general consensus was that is was 1.35 (presumably this means 1.35 g/cm^3 or 1350 mg/cm^3 since no units were given). It is known that the material is a combination of acrylic and poly-vinyl chloride (PVC).

Next, two series of 10 one-minute counts were taken on stainless steel shields currently in use, by the FSS team, in the performance of final status surveys. These shields are custom made for the Ludlum Model 44-116 thin plastic scintillation probe and they are designed such that the shield "snaps" onto the face of the 44-116 probe and holds itself in place. There are two thickness of shield: the thin shield is 0.018 inches thick (per the manufacturer) while the thick shield is 0.34 inches thick (as measured by calipers).

Lastly, three series of 10 one-minute counts were taken to check background.

5.0 ASSESSMENT

The graph of the original data in Appendix B appears to show two curves. It is apparent that the first curve, from 5.153 mg/cm^2 to 210.800 mg/cm^2 is the reduction of counts due to the combination of the 546 keV and 523.2 keV betas from Sr-90 and Y-90, respectively, while the remainder of the curve is due to the reduction in counts from the 2283.9 keV Y-90 beta.

In order to estimate the counts from the combination of the two low-energy betas, a least squares fit of the high-energy beta data is determined and extrapolated to 5.153 mg/cm^2.

The total counts minus the extrapolated counts result in the estimated low-energy beta count. Refer to Appendix C for the derivation of the least squares equations and Appendix D for the actual determination of least squares coefficients which are used to generate the extrapolated values.

5.1 Equations

The method of least squares [JOHN 1964, pp. 382-385, 399-400] was developed in Appendix C and a synopsis appears below. The equation $\ln y = a + bx$ is used to fit the existing data from Appendix B. The coefficients "a", "b", and "r" from Appendix C are repeated below.

$$a = \frac{\sum_{i=1}^{n} \ln y_i \sum_{i=1}^{n} x_i^2 - \sum_{i=1}^{n} x_i \ln y_i \sum_{i=1}^{n} x_i}{n\sum_{i=1}^{n} x_i^2 - \left(\sum_{i=1}^{n} x_i\right)^2} \qquad \textbf{(Eq. 5-1)}$$

$$b = \frac{n\sum_{i=1}^{n} x_i \ln y_i - \sum_{i=1}^{n} \ln y_i \sum_{i=1}^{n} x_i}{n\sum_{i=1}^{n} x_i^2 - \left(\sum_{i=1}^{n} x_i\right)^2} \qquad \textbf{(Eq. 5-2)}$$

$$r = \frac{n\sum_{i=1}^{n} x_i \ln y_i - \sum_{i=1}^{n} \ln y_i \sum_{i=1}^{n} x_i}{\sqrt{\left[n\sum_{i=1}^{n} x_i^2 - \left(\sum_{i=1}^{n} x_i\right)^2\right]\left[n\sum_{i=1}^{n} (\ln y_i)^2 - \left(\sum_{i=1}^{n} \ln y_i\right)^2\right]}} \qquad \textbf{(Eq. 5-3)}$$

5.2 Data Reduction

Appendix D shows the solutions for the equations shown in section 5.1. The equation $\ln y = a + bx$ now becomes $\ln y = 8.143 - 0.00448x$. In Table 5-1 below, the actual data and that predicted by the method of least squares are shown. Immediately below Table 5-1 is a graph showing pictorially how the two sets of data compare.

Table 5-1
Actual and Predicted 2283.9 keV Counts and Percent Difference

Range (mg/cm^2)	Actual 2283.9 keV Counts	Natural Log of 2283.9 keV Counts	Natural Log predicted by a + bx	Inverse Log Predicted by $y = e^{(a + bx)}$	% difference of Counts
210.800	1371.6	7.2237	7.1996	1338.9007	2.3840
279.349	990.9	6.8986	6.8927	985.0766	0.5877
347.897	705.2	6.5585	6.5858	724.7590	-2.7735
416.466	519.2	6.2523	6.2789	533.1831	-2.6932
484.995	388.8	5.9631	5.9721	392.3168	-0.9045
553.544	298.3	5.6981	5.6652	288.6413	3.2379
				average	-0.0269

Figure 5.1

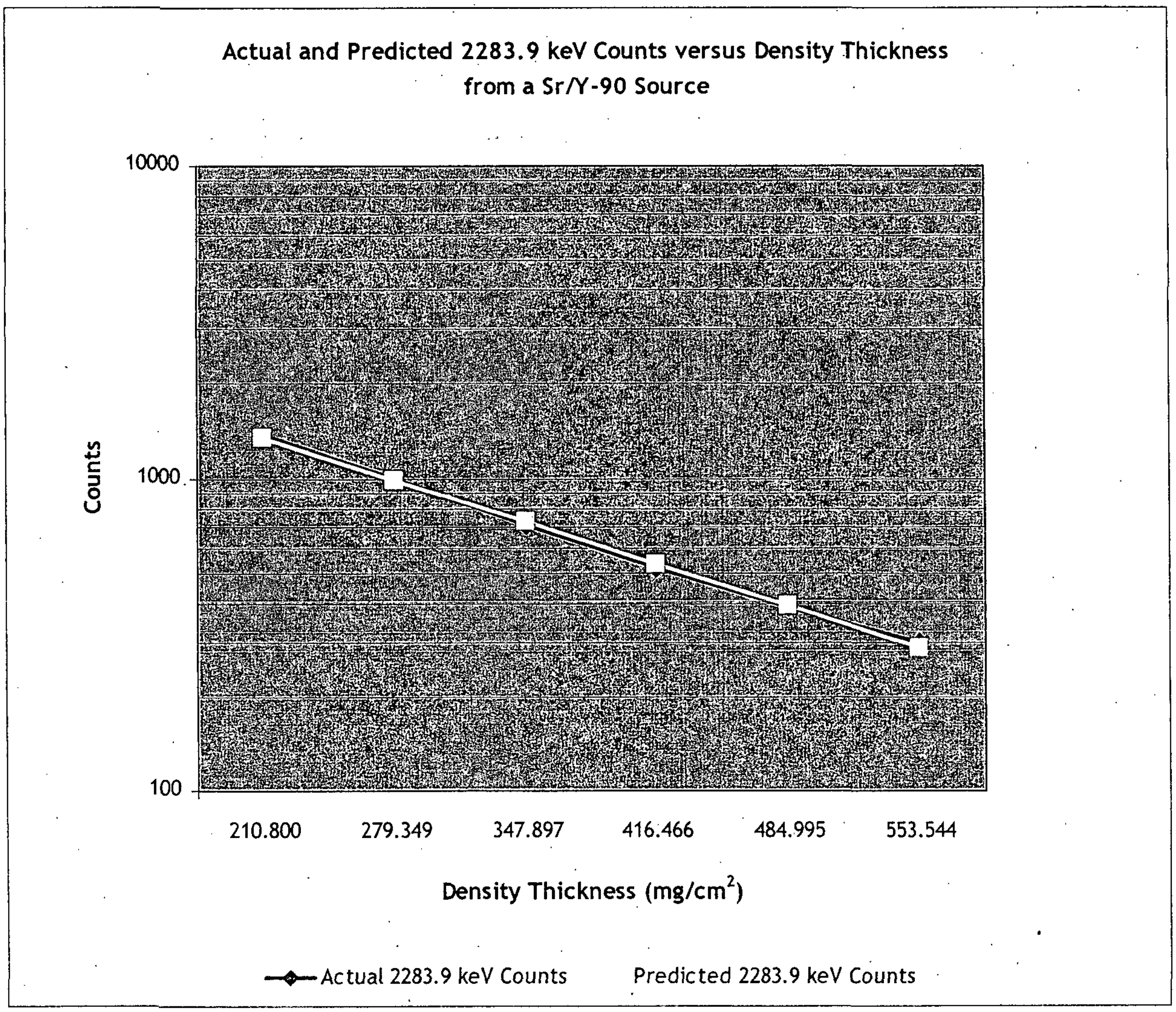

Over the linear portion of the curve, the data fit quite well as demonstrated by an r-squared value approaching unity. It is assumed that the reduction of counts due to the shielding is linear when plotted on semi-logarithmic paper. So one sees, from the graph in Appendix D, that the first curve is actually the reduction due to the combination of low-energy betas and the curve from 210.800 mg/cm^2 on is due to the presence of the high-energy beta.

5.3 Other Shield Materials

Performing interpolation of Appendix B, Acrylic/PVC combination data, it can be seen that the ¼"-thick material corresponds to a range of 649 mg/cm^2 while the ½"-thick material corresponds to a range of 827 mg/cm^2.

The expectation, after talking with McMaster-Carr, was that the ranges would be roughly 875 and 1680 mg/cm^2. These values are calculated below.

Range $_{¼"}$ = (0.255 in)(2.54 cm/in)(1350 mg/cm^3) = 875 mg/cm^2

Range $_{½"}$ = (0.49 in)(2.54 cm/in)(1350 mg/cm^3) = 1680 mg/cm^2

Since the density of the material was clearly not 1350 mg/cm^3, an attempt was made to calculate the density of the acrylic/PVC combination. Measurements are shown in Table 5-2 below.

Table 5-2
Measurements for ¼" and ½" Thick Pieces of Acrylic/PVC Material

Name	Mass (g)	Dimensions (inches)		
		length	width*	thickness*
¼" thick	227.6	12 3/32	4.99	0.255
½" thick	444.4	12 1/16	4.99	0.49

* width and thickness dimensions taken with digital caliper

Volume $_{¼"}$ = 15.38869 in^3 = 252.17548 cm^3
Volume $_{½"}$ = 29.49402 in^3 = 483.32037 cm^3

$$\rho_{1/4"} = \frac{(227.6g)\left(1000\frac{mg}{g}\right)}{252.17548cm^3} = 902.546\frac{mg}{cm^3} \qquad \textbf{(Eq. 5-4)}$$

$$\rho_{1/2"} = \frac{(444.4g)\left(1000\frac{mg}{g}\right)}{483.32037cm^3} = 919.473\frac{mg}{cm^3} \qquad \textbf{(Eq. 5-5)}$$

The average of the two pieces is approximately 910 mg/cm^3. Using the 910 mg/cm^3 density, the density thicknesses should have been 590 and 1132 mg/cm^2, respectively, for the ¼" and ½" thick material. As stated previously, density thicknesses of 649 mg/cm^2 and 827 mg/cm^2 were calculated from interpolating the data obtained on 12/18/07.

Performing interpolation of Appendix B, Stainless Steel data, it can be seen that the thin shield corresponds to a density thickness of 445 mg/cm^2 while the thick shield corresponds to a density thickness of 731 mg/cm^2. The density of the thin shield was quoted by Ludlum as 7.9292 kg/m^3 [LMI 2007]. The thick shield was not manufactured by Ludlum. Using the Range-Energy equation from Section 2.2, it can be seen that the two shields are calculated to be 363 mg/cm^2 and 685 mg/cm^2. This agreement, although closer than the acrylic-PVC combination, is still not that close.

5.4 Bremsstrahlung Production

The effect of bremsstrahlung production on the measurement of Sr/Y-90 beta absorption is examined. Bremsstrahlung are x-rays that are emitted when high-speed, charged particles undergo rapid deceleration. When a beta particle passes close to a nucleus, the strong attractive coulomb force causes the beta particle to deviate from its original path. The change in direction is due to a radial deceleration and the beta particle loses energy by electromagnetic radiation. This means that the bremsstrahlung photons have a continuous energy distribution that ranges downward from the theoretical maximum equivalent to the kinetic energy of the beta particle.

For the purposes of estimating, the following equation [CEM 1983, p. 106] can be used

$$f = 3.5x10^{-4} ZE \qquad \textbf{(Eq. 5-6)}$$

where: $f \equiv$ fraction of the incident beta energy converted into photons
$Z \equiv$ atomic number (the number of protons in the nucleus) of the absorber
$E \equiv$ maximum energy of the beta particle in MeV

Because bremsstrahlung production increases with the atomic number of the absorber, beta shields are generally made with materials containing the minimum possible atomic number. Practically speaking, beta shields of atomic number greater than 13 (aluminum) are seldom used. Presumably, the reason stainless steel is used on the Ludlum Model 44-116 probe is because the plastic scintillator, from which the detector is manufactured, is thin enough that the bremsstrahlung photons pass through the material without interaction. But, since bremsstrahlung photons are emitted in a continuous energy spectrum, the lower energy photons will interact with the scintillation material and, therefore, cause additional counts to be measured.

To illustrate, the shields currently used in final status surveys are constructed of stainless steel with a Z of approximately 26 (Iron). In actuality, the value of Z is a little greater than 26 owing to the presence of Nickel with Z equal to 28. Using the values from Table 2-1, it can be seen that the fraction of beta energy converted into photons is

$f_{546} = (3.5x10^{-4})(26)(0.546) = 4.97x10^{-3}$, **(Eq. 5-7)**

$f_{523.2} = (3.5x10^{-4})(26)(0.5232) = 4.76E-3$, and **(Eq. 5-8)**

$f_{2283.9} = (3.5x10^{-4})(26)(2.2839) = 2.08E-2$. **(Eq. 5-9)**

The flux of bremsstrahlung photons [CEM 1983, p. 107].is calculated using the equation

$$\phi = \frac{fE_\beta}{4\pi r^2 E} \quad \textbf{(Eq. 5-10)}$$

where: $f \equiv$ fraction of the incident beta energy converted into photons
$E_\beta \equiv$ total beta energy in MeV per unit time (based on Table 2-1), this is the average energy of the beta particles multiplied by the probability of the beta emission multiplied by the number of betas per unit time
$E \equiv$ maximum energy of the beta particle (for health physics purposes, it is assumed that all bremsstrahlung photons are of the maximum energy so this variable has units of MeV/photon)
$r \equiv$ distance from the source in centimeters

To obtain E_β, the total beta energy, the number of atoms of Sr-90 and Y-90 on 12/18/07 must be known. The source certificate indicates a Sr-90 activity of 0.01383×10^{-6} Curies (30,702.6 dpm or 511.71 dps) on 11/1/83. The elapsed time between 11/1/83 and 12/18/07 is 8813 days.

The equations (CEM 1983, pp. 91-92) used to calculate the parent and daughter activities at any time "t" are shown below. Subscripts "A" and "B" refer to the parent and daughter radionuclide, respectively.

$A_A = \lambda_A N_{A_0} = A_{A0} e^{-\lambda_A t}$ activity of parent at any time "t" **(Eq. 5-11)**

$A_B = \lambda_B N_B = \dfrac{\lambda_B(\lambda_A N_{A_0})}{\lambda_B - \lambda_A}\left[e^{-\lambda_A t} - e^{-\lambda_B t}\right]$ activity of daughter at any time "t" **(Eq. 5-12)**

$$\lambda_A = \frac{\ln 2}{T_{A\frac{1}{2}}} = \frac{\ln 2}{(28.6yr)\left(365.25\dfrac{days}{yr}\right)} = \frac{6.635E-5}{day} \quad \textbf{(Eq. 5-13)}$$

$$\lambda_B = \frac{\ln 2}{T_{B\frac{1}{2}}} = \frac{\ln 2}{(64.1hrs)\left(\dfrac{1day}{24hrs}\right)} = \frac{2.595E-1}{day} \quad \textbf{(Eq. 5-14)}$$

$$A_A = 30{,}702.6dpm\left[e^{-\left(\frac{6.635E-5}{day}\right)(8813days)}\right] = 17{,}108.4dpm \qquad \textbf{(Eq. 5-15)}$$

$$A_B = \frac{30{,}702.6dpm}{\frac{2.595E-1}{day} - \frac{6.635E-5}{day}}\left[e^{-\left(\frac{6.635E-5}{day}\right)(8813days)} - e^{-\left(\frac{2.595E-1}{day}\right)(8813days)}\right] = 17112.7dpm \qquad \textbf{(Eq. 5-16)}$$

On 12/18/07, the decayed Sr-90 activity is 17,108.4 dpm (285.1 dps), while the Y-90 daughter activity in growth is 17112.7 dpm (285.2 dps). The total Sr-90 plus Y-90 activity on 12/18/07 is 34,221.1 dpm (570.4 dps). As an aside, notice how the source actually has more activity 8813 days later than it did when it was originally manufactured.

Now getting back to the bremsstrahlung flux equation, it can be seen that with the source-to-probe distance of 0.97875 inches (2.486025 cm) the bremsstrahlung photon flux becomes

$$\phi_{546} = \frac{\left[4.97x10^{-3}\right]\left[\left(0.1958\frac{MeV}{\beta}\right)\left(1.000\frac{\beta}{dis}\right)\left(285.1\frac{dis}{\sec}\right)\right]}{4\pi(2.486025cm)^2\left(0.546\frac{MeV}{photon}\right)} = 6.54x10^{-3}\frac{photons}{cm^2-\sec}$$

(Eq. 5-17)

$$\phi_{523.2} = \frac{\left[4.76E-3\right]\left[\left(0.1865\frac{MeV}{\beta}\right)\left(0.000115\frac{\beta}{dis}\right)\left(285.2121\frac{dis}{\sec}\right)\right]}{4\pi(2.486025cm)^2\left(0.5232\frac{MeV}{photon}\right)} = 7.17x10^{-7}\frac{photons}{cm^2-\sec}$$

(Eq. 5-18)

$$\phi_{2283.9} = \frac{\left[2.08x10^{-2}\right]\left[\left(0.9348\frac{MeV}{\beta}\right)\left(0.99989\frac{\beta}{dis}\right)\left(285.2121\frac{dis}{\sec}\right)\right]}{4\pi(2.486025cm)^2\left(2.2839\frac{MeV}{photon}\right)} = 3.12x10^{-2}\frac{photons}{cm^2-\sec}$$

(Eq. 5-19)

$$\phi_{total} = 3.78x10^{-2}\frac{photons}{cm^2-\sec} \quad \text{or} \quad \phi_{total} = 2.27\frac{photons}{cm^2-\min} \qquad \textbf{(Eq. 5-20)}$$

As a worst-case scenario, assume that the bremsstrahlung photons are emitted right from the source and that they scatter from an initial source diameter of 1 5/8" into a detector diameter of 9.10 cm. The 9.10 cm diameter is subtended by the 45 degree angle about the entire edge of the source diameter (see Figure 5.2 below). Assume also that the distance the photons must travel to the outer edge of the detector (4.05 cm which is the $\sqrt{2}$ times the straight line distance of 2.486025 cm) is neglected. Assume further that because the plastic scintillator in the Ludlum Model 44-116 probe is 0.010 inches thick [LMI 2006], the efficiency of detection is one percent or less.

Figure 5.2

BREMSSTRAHLUNG PATH
FROM SOURCE TO 44-116 PROBE

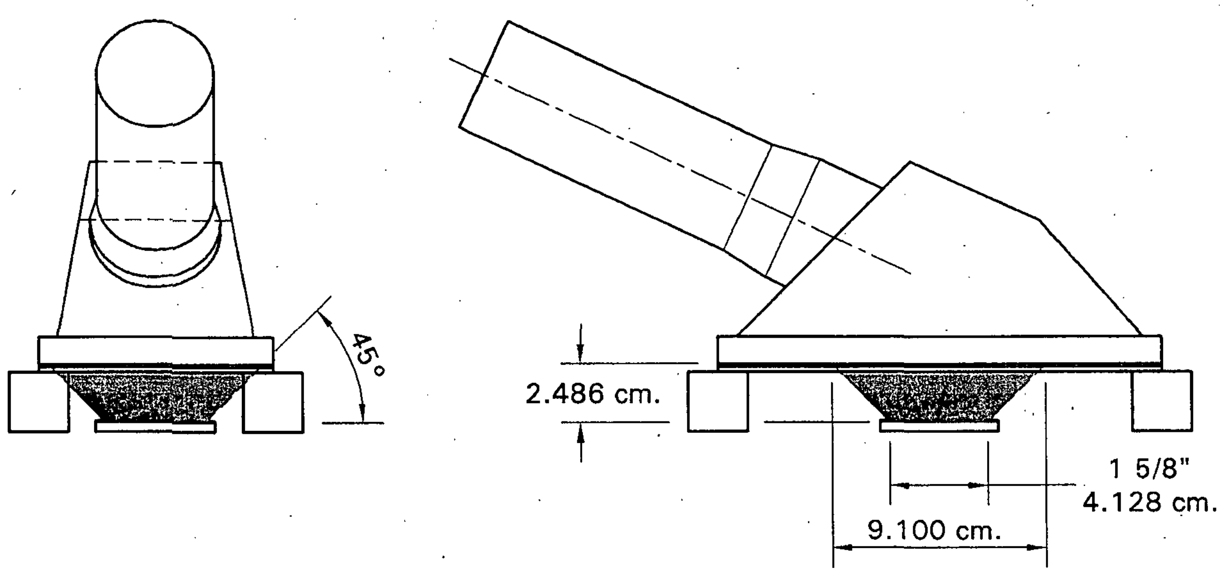

The number of photons per minute counted by the probe becomes the product of the bremsstrahlung flux, the affected area of the probe surface, and the detection efficiency.

$$\phi_{total} A = \left[2.27 \frac{photons}{cm^2 - \min}\right]\left[\frac{\pi (9.9cm)^2}{4}\right][0.01] = 1.5 \frac{photons}{\min} \qquad \textbf{(Eq. 5-21)}$$

On inspection, one determines rather quickly that the number of bremsstrahlung photons counted is insignificant when compared to the average background counts of 150 and a standard deviation of 15.4 counts over a one minute interval (see Appendix B).

Since aluminum has Z=13, the bremsstrahlung photon flux would be half of that from stainless steel. From the acrylic/PVC combination, the flux would be expected to be even less than that obtained from aluminum.

6.0 CONCLUSIONS

The purpose of this document was to confirm the range of beta particles in aluminum, using a Ludlum Model 44-116 plastic scintillation probe, and then to determine the amount of shielding material needed to completely block all Sr/Y-90 betas from residual surface contamination. This is to ensure that Ludlum Model 44-116 unshielded readings (beta plus gamma) minus shielded readings (gamma only) provide the true beta-only response in the limiting case where Sr/Y-90 is the predominant beta-emitter present.

Data were obtained by placing successive 0.010-inch-thick layers of aluminum sheet between a Sr/Y-90 source and the probe and plotting the exponential reduction in counts. In addition, both probe shields (thin and thick stainless steel) currently utilized on the project and three different thicknesses of PVC were placed between the source and probe and the measurements were documented. Interpolation of the aluminum shield count data, with the counts collected with the stainless steel and PVC, was done to calculate the density thicknesses of the stainless steel and PVC.

Equation 4-2 does not take into consideration the effect of relative humidity on the density of air. The correct density equation for humid air [WIKI 2008] is shown below.

$$\rho_{air} = \frac{P_d}{R_d T} + \frac{P_v}{R_v T} \qquad \textbf{(Eq. 6-1)}$$

where: $P_d \equiv$ atmospheric pressure in Pascals (1 mbar = 100 Pascals and 1 Pa = 1 N/m^2)

$R_d \equiv$ specific gas constant 287.05 J/kg-^{o}K (for dry air)

$T \equiv$ absolute temperature in degrees Kelvin

$P_v \equiv$ vapor pressure of water in Pascals

$R_v \equiv$ specific gas constant 461.495 J/kg-^{o}K (for water vapor)

$\rho_{air} \equiv$ density of air in kg/ m^3 (or mg/cm^3)

$^{0}K \equiv 273.15 + \frac{5}{9}\left({}^{0}F - 32\right)$

$$P_v = \phi \cdot P_{sat} \qquad \textbf{(Eq. 6-2)}$$

where: $\phi \equiv$ relative humidity (in decimal form)

$P_{sat} \equiv$ saturation vapor pressure in mbars (1 mbar = 100 Pascals)

$$P_{sat} = 6.1078x10^{\frac{7.5T-2048.625}{T-35.85}} \qquad \textbf{(Eq. 6-3)}$$

By substituting 60 degrees Fahrenheit (288.71 °K), P_{sat} becomes 17.67 millibars, P_v becomes 1767 Pa (assuming 100% humidity and 100 Pa per millibar), and $\frac{P_v}{R_v T}$ becomes 0.013 kg/m^3. Compared to the density calculated by equation 4.2 (1.229 kg/m^3), this represents only a one percent difference. Further, since it is related to air, this represents only a one percent change in the density thickness of air. From Section 4.2, the density thickness of air is 3.053 mg/cm^2. A one percent increase amounts to 0.03 mg/cm^2: insignificant, especially when compared to the range of betas under consideration in this analysis.

The density thickness of the ¼" acrylic/PVC shield is 649 mg/cm^2 while the ½" acrylic/PVC shield is on the order of 827 mg/cm^2.

The thin stainless steel shield equates to roughly 445 mg/cm^2 while the thick shield would be roughly 731 mg/cm^2. Using the Range-Energy equation from Section 2.2, it can be seen that the density thicknesses of the two shields are calculated to be 363 mg/cm^2 and 685 mg/cm^2 for the thin and thick stainless steel shields, respectively.

From the graph in Appendix D, it is clear that a density thickness of 180 mg/cm^2 is more than enough to block the low-energy betas from the 44-116 probe, while a density thickness of 1100 mg/cm^2 is adequate to completely block all of the high energy beta particles from Y-90. The values of 180 mg/cm^2 and 1100 mg/cm^2 are chosen from Table 2-1.

It would appear that using multiple sheets of aluminum instead of single-piece absorbers made for more effective count reduction than would have been expected. This is most likely due to the betas having to pass multiple air-aluminum interfaces rather than passing through a single thickness of aluminum as would have occurred if a set of absorbers could have been procured.

For this probe/source/shield setup, bremsstrahlung production is insignificant, though it should not be overlooked when performing these types of analyses. The error bars on the background measurements are larger than the calculated contribution from bremmstrahlung photons to the overall count rate. In short, the bremsstrahlung contribution is "buried in the noise".

The stainless steel shields presently in use for final status surveys do not meet the procedure CS-01, step 4.3.3.5, criterion of 900 mg/cm^2. Not trying to downplay the seriousness of this fact, but Sr-90 does not play a significant role in the beta DCGLs in use on this site. Further, it is not possible on this site to accurately measure how many beta particles are emitted with energies greater than that needed to be stopped by the thick stainless shield (731 mg/cm^2). Be that as it may, it is recommended that the FSS organization procure shields with a density thickness of at least 900 mg/cm^2 in order to be sure of blocking most of the Y-90 betas from shielded counts and obtaining more accurate beta plus gamma and gamma-only measurements. In addition, the new shields should be made of aluminum or some hydrogenous-equivalent material, like polycarbonate (Lexan), polymethyl methacrylate (Lucite, Plexiglass), polyvinyl chloride (PVC), Acrylic, or other low-Z material in order to cut down on the production of bremsstrahlung photons. Dividing the required density thickness by the density of a specific material yields the thickness of material needed. With a density 2700 mg/cm^3, 900 mg/cm^2 represents an Aluminum thickness of 0.3333 cm (0.1312 inches). For Acrylic-PVC, with density of 910 mg/cm^3, 900 mg/cm^2 corresponds to a thickness of 0.9890 cm (0.3894 inches). For Acrylic-PVC, with density of 1350 mg/cm^3, 900 mg/cm^2 corresponds to a thickness of 0.6667 cm (0.2625 inches).

7.0 APPENDICES

Appendix A – Source Certification, Photographs of Source, Scale Drawing of Setup, Photographs of Source and Probe Orientation
Appendix B – Data Obtained from a Ludlum Model 44-116 Plastic Scintillation Probe
Appendix C – Derivations of Equations
Appendix D – Determination of Coefficients

APPENDIX A

(13 pages total)

Source Certification

(4 pages)

Photographs of Source

(2 pages)

Scale Drawing of Setup

(1 page)

Photographs of Source and Probe Orientation

(5 pages)

RADIOACTIVE MATERIAL RECEIPT AND INVENTORY RECORD

☐ SNM ☒ B-P ☐ SM ☐ OTHER

IDENTIFICATION NO.	DATE INVENTORIED	DATE DISPOSED
	12-12-83	

ORDERING INFORMATION

RADIOISOTOPE: Strontium-90	QUANTITY (gms/lbs)	ACTIVITY (Curies)
CHEMICAL FORM	PHYSICAL FORM/SIZE: solid- standard source	$T_{\frac{1}{2}}$: 28.9 yr
RADIATION: beta	INTENDED USE: calibration of HP instruments	
PURCHASE REQ. NO.: 508729	ORDER/CONTRACT NO.: C-82187-D	LICENSE NO.
SECT. ACCT./ACCT. OFFICER	RESPONSIBLE USER: Health Physics	ORDERED BY AND DATE: B. King
VENDOR: Isotopes Products Lab.	H.P. & L. REVIEW BY AND DATE	

DESCRIPTION

RADIOISOTOPE: Strontium-90	CHEMICAL FORM	ACTIVITY (Curies): 0.01383×10^{-6} 11-1-83
PHYSICAL FORM: solid	NET WT. COMPOUND (gms/lbs)	% ELEMENT IN COMPOUND
NET WT. ELEMENT (gms/lbs)	% ISOTOPE IN ELEMENT	NET WT. ISOTOPE (gms/lbs)

TYPE ENCAPSULATION: evaporated metallic salts covered with mylar film

REMARKS:
Source No. F-331
Stainless steel backed; ~~1~~5/8" active diameter

HEALTH PHYSICS SURVEY

SURVEYED AT RECEIVING (Signature and Date): delivered to Environ. Health Branch 12-8-83

TYPE SHIPPING CONTAINER: fibreboard box- USA DOT 7A Type A

SHIPPING CONTAINER SURVEY

1. MAXIMUM EXTERNAL RADIATION LEVEL	2. TRANSFERRABLE CONTAMINATION ON OUTER SURFACE
0 mrem/hr at outer surface	4 d/m/100 cm2 alpha
0 mrem/hr at 3 ft. from outer surface	8 d/m/100 cm2 beta-gamma
RECEIVED AT M&S (Date): 12-9-83	USER NOTIFIED (Date)

BARE SOURCE RADIATION SURVEY: ~~certified source activity: 3.07×10^4 dpm~~

APPLICABLE RESTRICTIONS: ~~Do not touch source surface~~

ACCOUNTABILITY

STORAGE LOCATION	USE LOCATION
~~Bldg. 49, Rm 17~~ B.140 hall	~~Bldg. 49, Rm 17~~

CUSTODY ASSUMED BY (Signature and Date)

1. Health Physics- DAK 12/9/83	3.
2.	4.

COPY DISTRIBUTION: WHITE - Health Physics Receipt File; PINK - Responsible User; CANARY - Health Physics Inventory File; GOLDENROD - Sec. Acct./Accountability Officer

Physical inventory 9-27-89 Bldg 49 Rm 17 DAK

NASA-C-811 (Rev. 3-71) NASA-Lewis

CERTIFICATE OF RADIOACTIVITY CALIBRATION

Isotope: Sr-90 Half-Life: 28.82 ± 0.14 y

Source No.: F - 331

Was assayed as containing: 13.83 nCi (3.07×10^4 dpm)

As of: 11-1-83

METHOD OF CALIBRATION:

( ) The source was assayed on a 3" x 3" NaI (Tl) crystal in conjunction with a single-channel analyzer, using the MeV peak (a value of gamma rays per decay was used in the calculations), against standard No. , in the same geometrical arrangement.

(✓) The source was assayed in an internal proportional/~~large area, low background~~ counter against Sr-90 standard No. 19122-3

( ) The source was assayed by alpha spectrometry on a surface barrier detector in conjunction with a single-channel analyzer, against standard No. in the same geometrical arrangement.

(✓) The source was prepared from a weighed aliquot of a solution whose activity in uCi/gm was determined by the method indicated above.

( )

ERROR CALCULATION:

a) Uncertainty due to systematic errors:
1. In assay of standard: ± 2.2 %
2. In weighing(s): ± 1.0 %

b) Uncertainty due to random errors:
Precision of source count, e_1; standard count e_2 and background count e_3:
$= \pm t \sqrt{e_1^2 + e_2^2 + e_3^2} = \pm$ 2.3 %

c) Total uncertainty:
TU = a + b = ± 5.5 %

NOTES

IPL participates in a NBS measurement assurance program to establish and maintain implicit traceability for a number of nuclides, based on the blind assay (and later NBS certification) of Standard Reference Materials. (As in NRC Regulatory Guide 4.15)

(✓) The total uncertainty is calculated at the 99 % confidence level.

(✓) This calibration is ~~directly~~/indirectly based on NBS Standard Reference Material No. 4919 D Sr-90

Vasana Nibhatabadya

Quality Control

ISOTOPE PRODUCTS LABORATORIES
1800 No. Keystone St., Burbank, California 91504

LEAK TEST CERTIFICATE

CUSTOMER NASA LEWIS RES. CTR. P.O.= C-82187-D

CATALOG = LB-90, LB-137, LB-60 CAPSULE TYPE 2" Planchet S/N F-331, F-332, F-333

RADIONUCLIDE Sr 90, Cs 137, Co 60 NOMINAL ACTIVITY 3x10⁴ dpm each.

THE LEAK TESTS INDICATED BY THE CHECKED BOXES WERE APPLIED TO DETERMINE THE INTEGRITY OF THE SOURCE(S) IN THIS SHIPMENT.

☒ 1. **STANDARD WIPE TEST**

The source is swabbed over its entire surface with a moistened paper or cotton swab. After being allowed to dry, the swab is counted using a windowless gas flow proportional counter. Activity levels exceeding 0.005 microcuries will be cause for rejection.

Measured Activity: <0.001 μCi ~~alpha~~ beta gamma

☐ 2. **BUBBLE TEST**

The source is immersed in ethylene glycol to a depth of 2" in a glass container and a vacuum of 10 cm or less applied. A steady stream of bubbles from the window or weld detail will be cause for rejection.

☐ 3. **SOAK TEST**

The source is immersed in distilled water and maintained at 50°C for a 4 hour period or overnight at room temperature. After removal of the source the liquid is evaporated in a planchet and the dry residue counted in a windowless proportional flow counter. Activity levels exceeding 0.005 μCi will be cause for rejection.

Measured Activity: μCi alpha beta gamma

☐ 4. **GAS SOURCE TEST (Radioactive Gases)**

The source is placed in a vacuum desiccator or similar chamber, evacuated to less than 1 mm. and left for a period of approximately fourteen hours. Air is introduced into the chamber and the air monitored with an end window G.M. tube. Readings exceeding 1000 CPM will be cause for rejection of the source.

☐ 5. **LEAK TEST NOT APPLICABLE**

The active area of this source is uncovered or protected by a very thin coating. Although the deposit is adherent, it is not designed or certified to pass a standard leak test. The inactive portions of the source have been checked using the standard wipe test and found not to exceed 0.005 μCi of removable activity at time of shipment.

Date 1 Dec 1983

Edward C. B[signature]
Health Physicist

ISOTOPE PRODUCTS LABORATORIES
1800 N. Keystone Street
Burbank, California 91504

ISOTOPE PRODUCTS LABORATORIES 1800 NO. KEYSTONE ST. BURBANK, CALIFORNIA 91504
(213) 843-7000

DATA SHEET

CUSTOMER: NASA LEWIS RES CTR. P.O.# C-82187-D DATE: 1 Dec. 1983

CATALOG # LB-90, LB-137, LB-60 QUANTITY: 3

CAPSULE TYPE: 2" planchets

NATURE OF ACTIVE DEPOSIT: Uniformly distributed and evaporated metallic salts.

ACTIVE DIAMETER: 1 5/8"

BACKING: 0.01" Stainless Steel

COVER: 0.9 mg/cm² mylar film

ISOTOPE	SOURCE #	ACTIVITY	CALIB. DATE	UNCERTAINTY
Sr 90	F-331	13.83 nCi (3.07×10^4 dpm)	11-1-83	± 5.5%
Cs 137	F-332	16.55 nCi (3.67×10^4 dpm)	12-1-83	± 3.1%
Co 60	F-333	16.71 nCi (3.71×10^4 dpm)	12-1-83	± 2.9%

REMARKS:
Leak Test and Calibration Certificates enclosed.

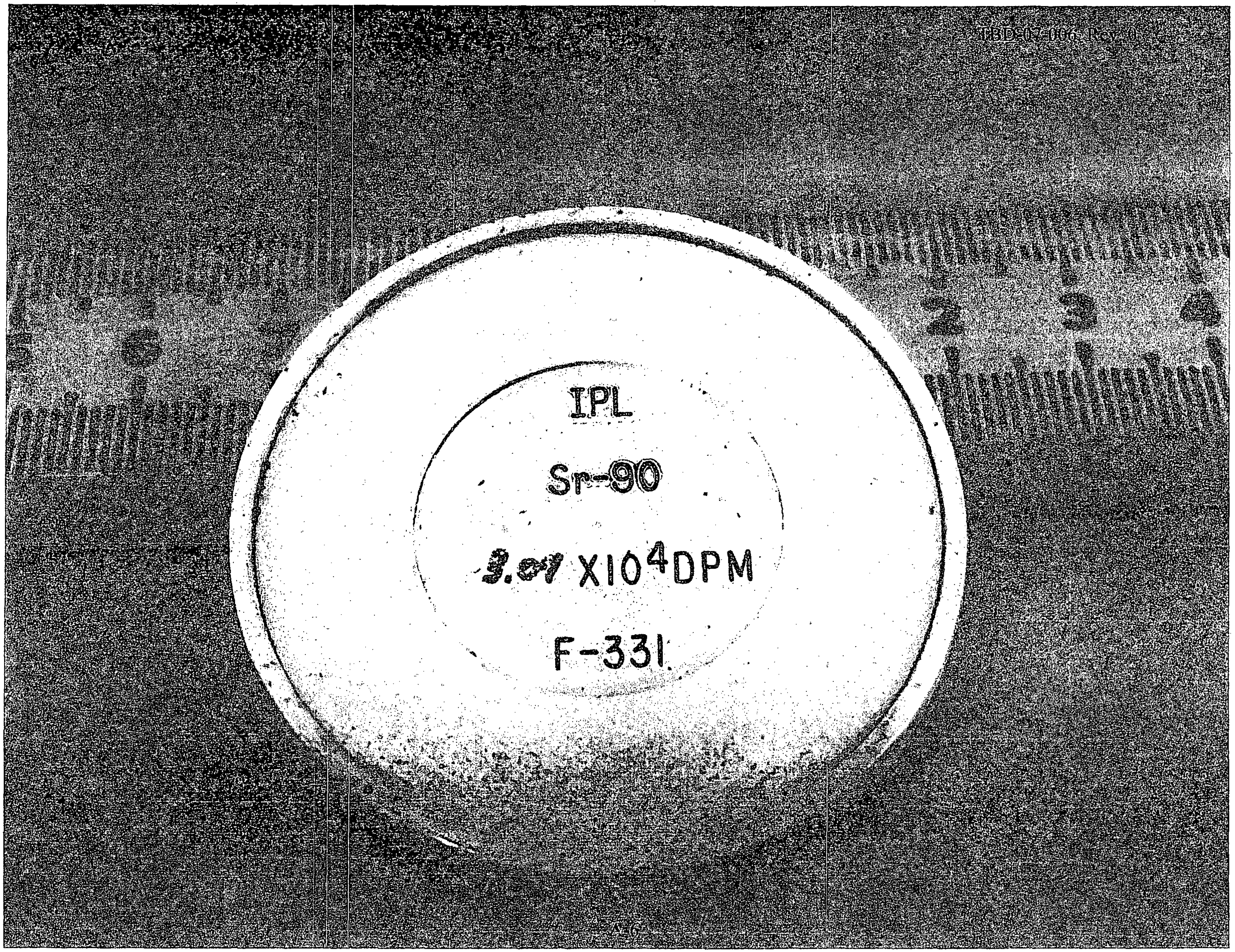
IPL
Sr-90
3.01 X10^{4}DPM
F-331

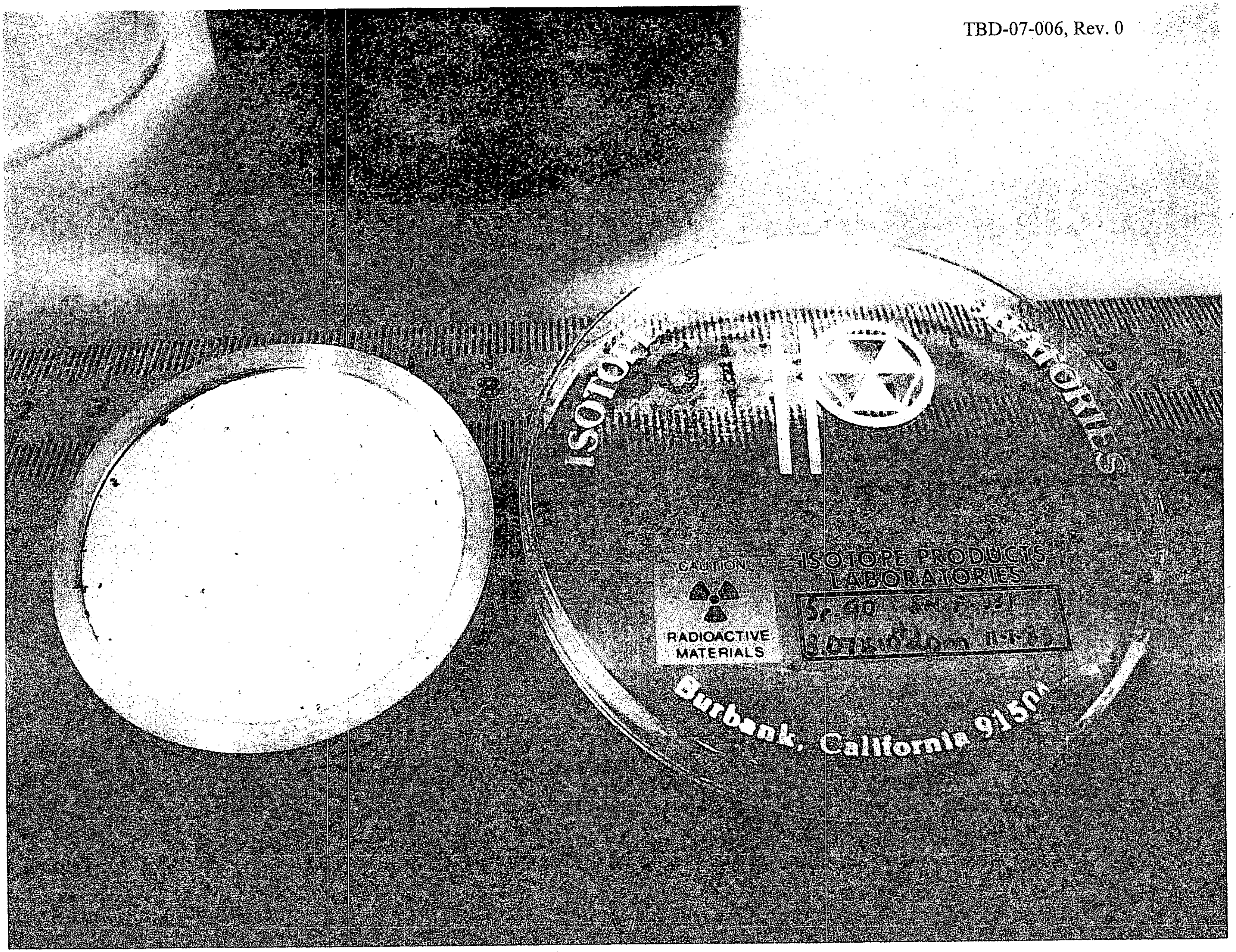
ISOTOPE PRODUCTS
LABORATORIES
CAUTION
RADIOACTIVE
MATERIALS
Sr-90
Burbank, California

SCALE DRAWING OF PROBE SOURCE SETUP

LUDLUM MODEL
44-116 PROBE

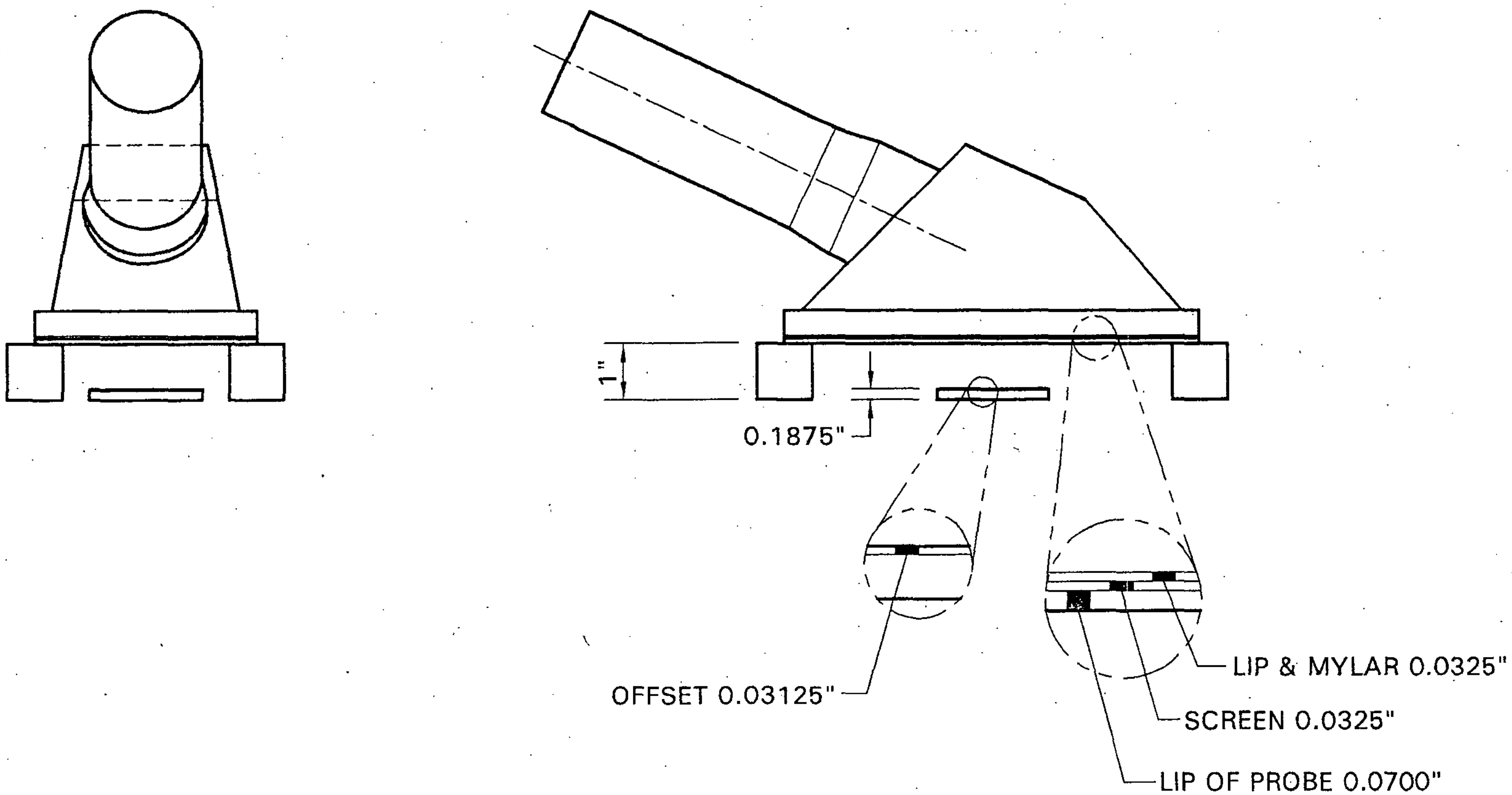

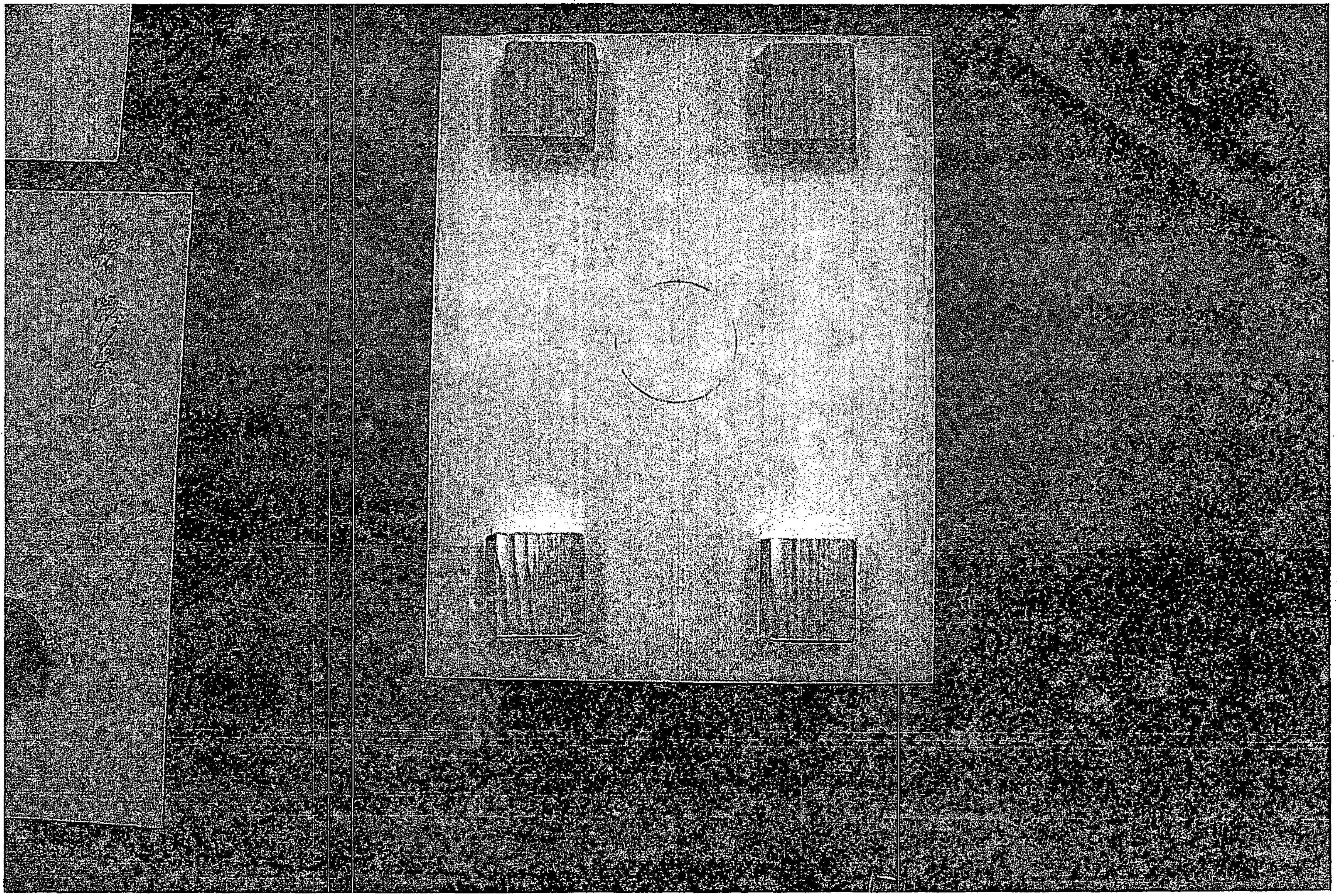

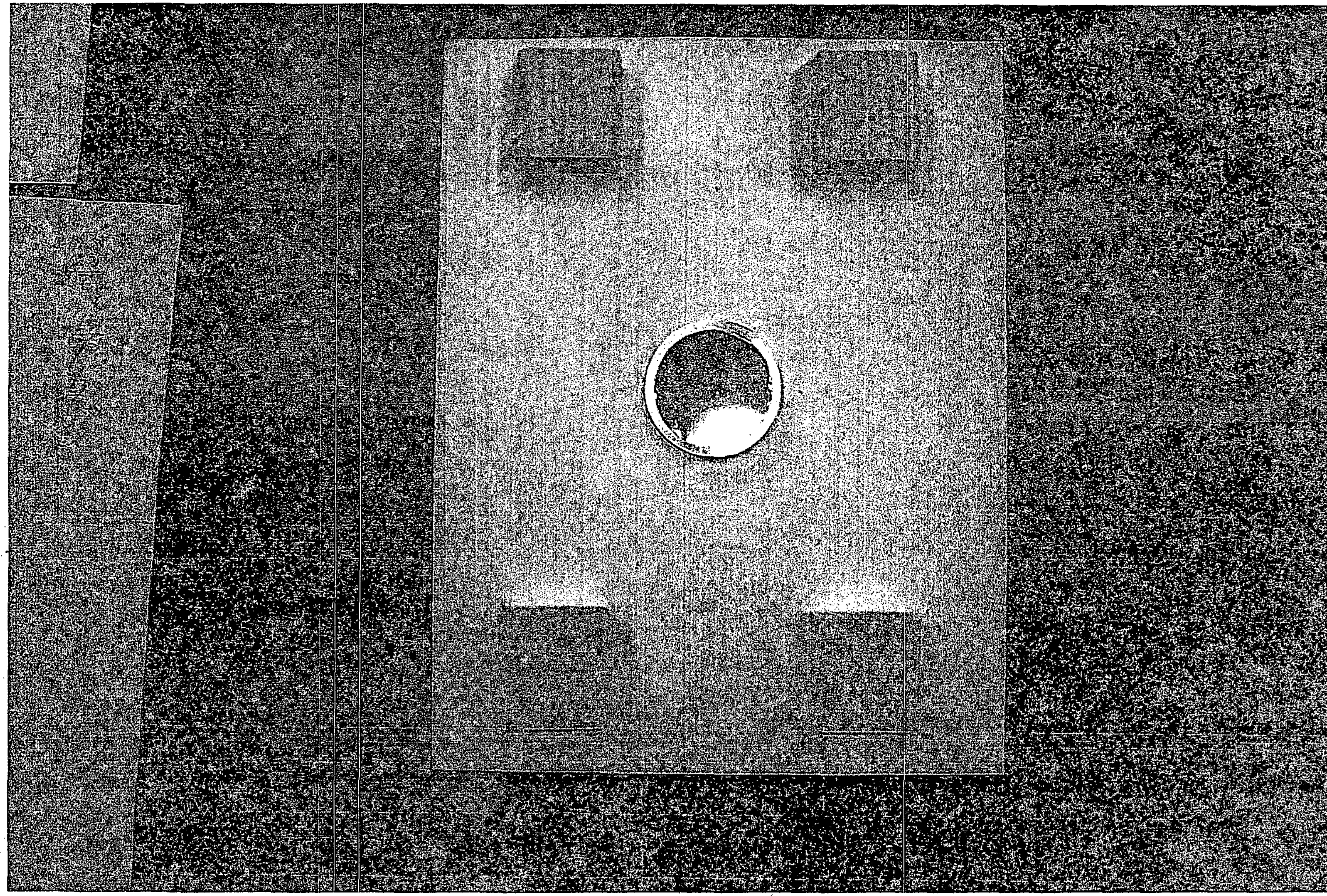

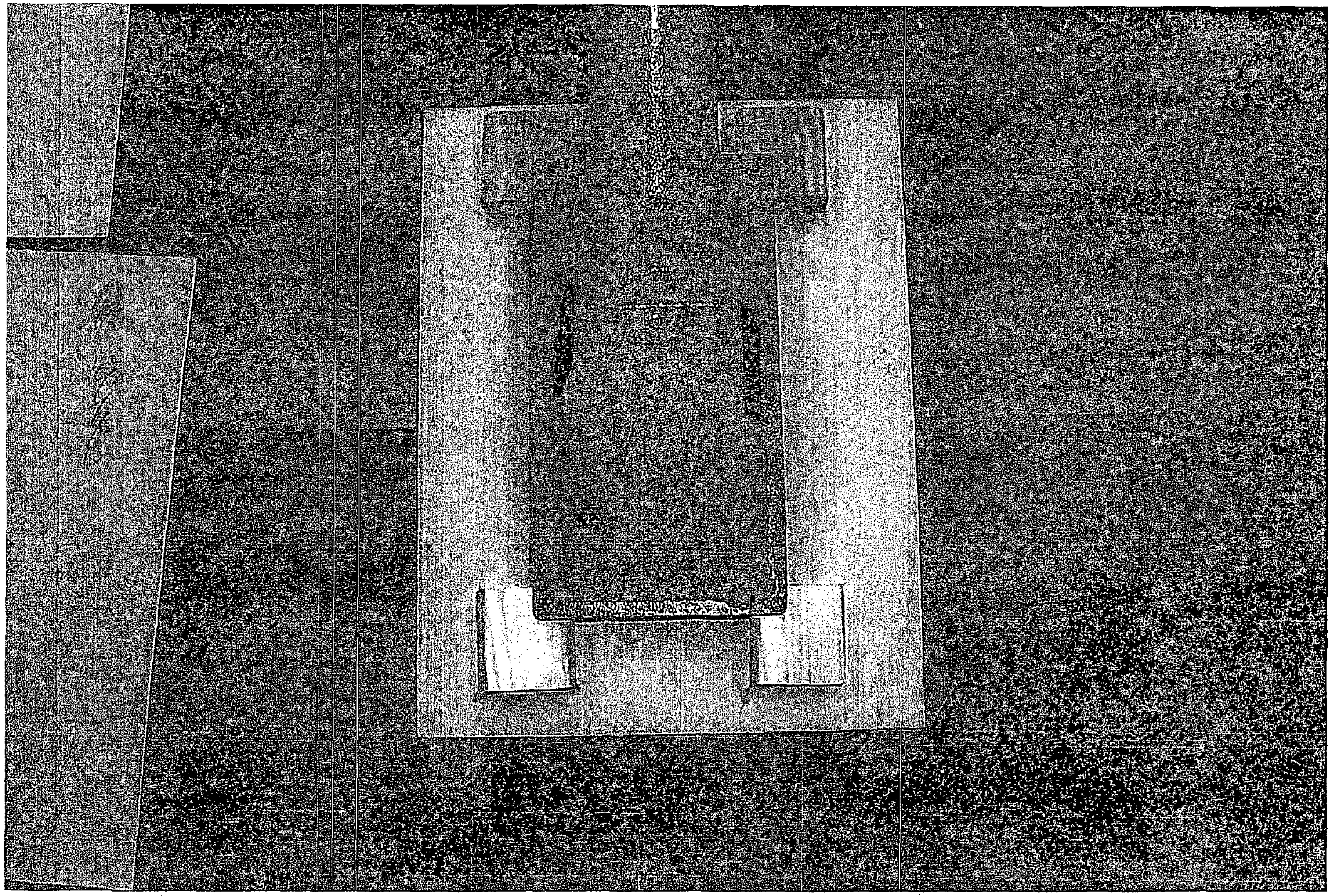

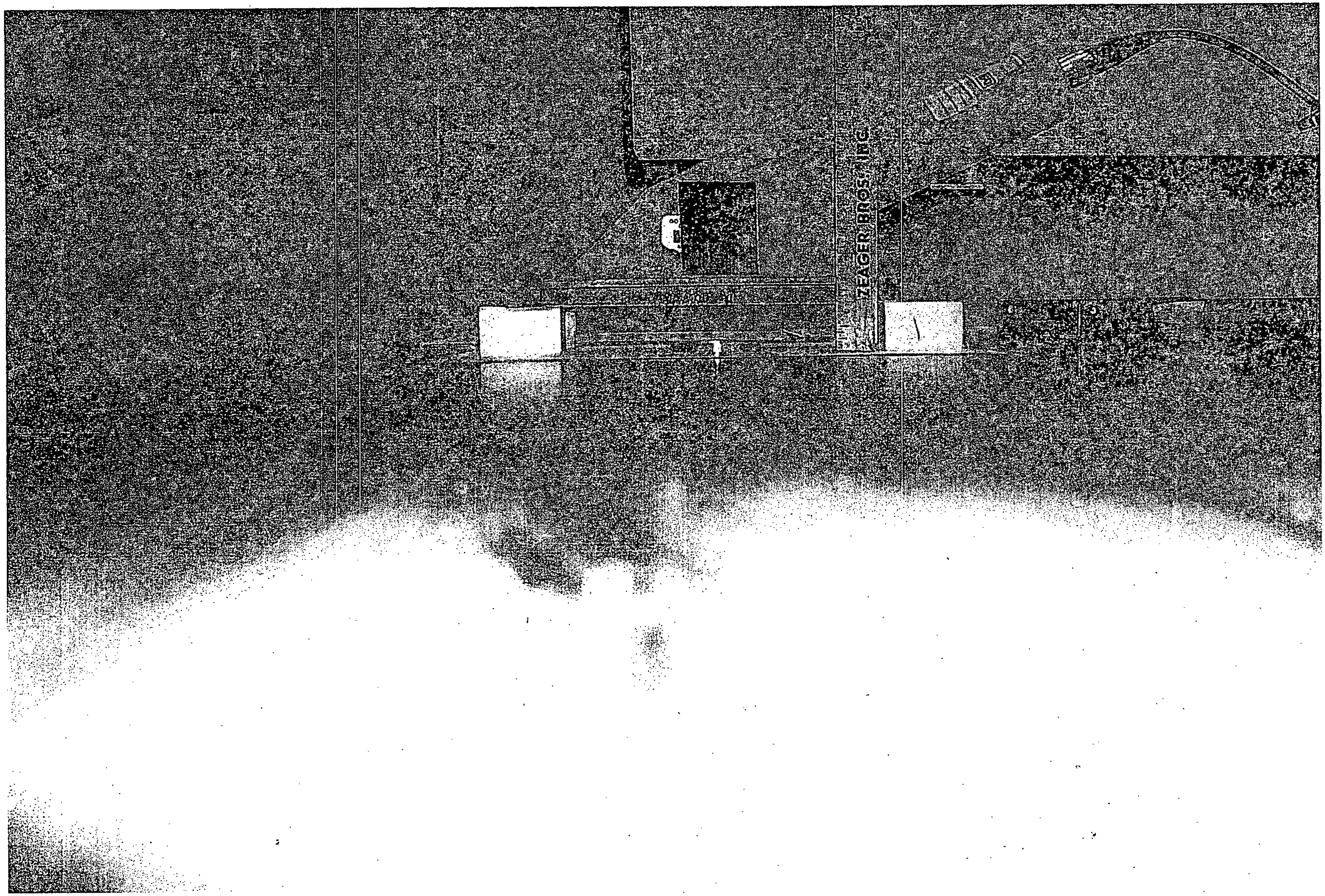
ZEAGER BROS. INC.

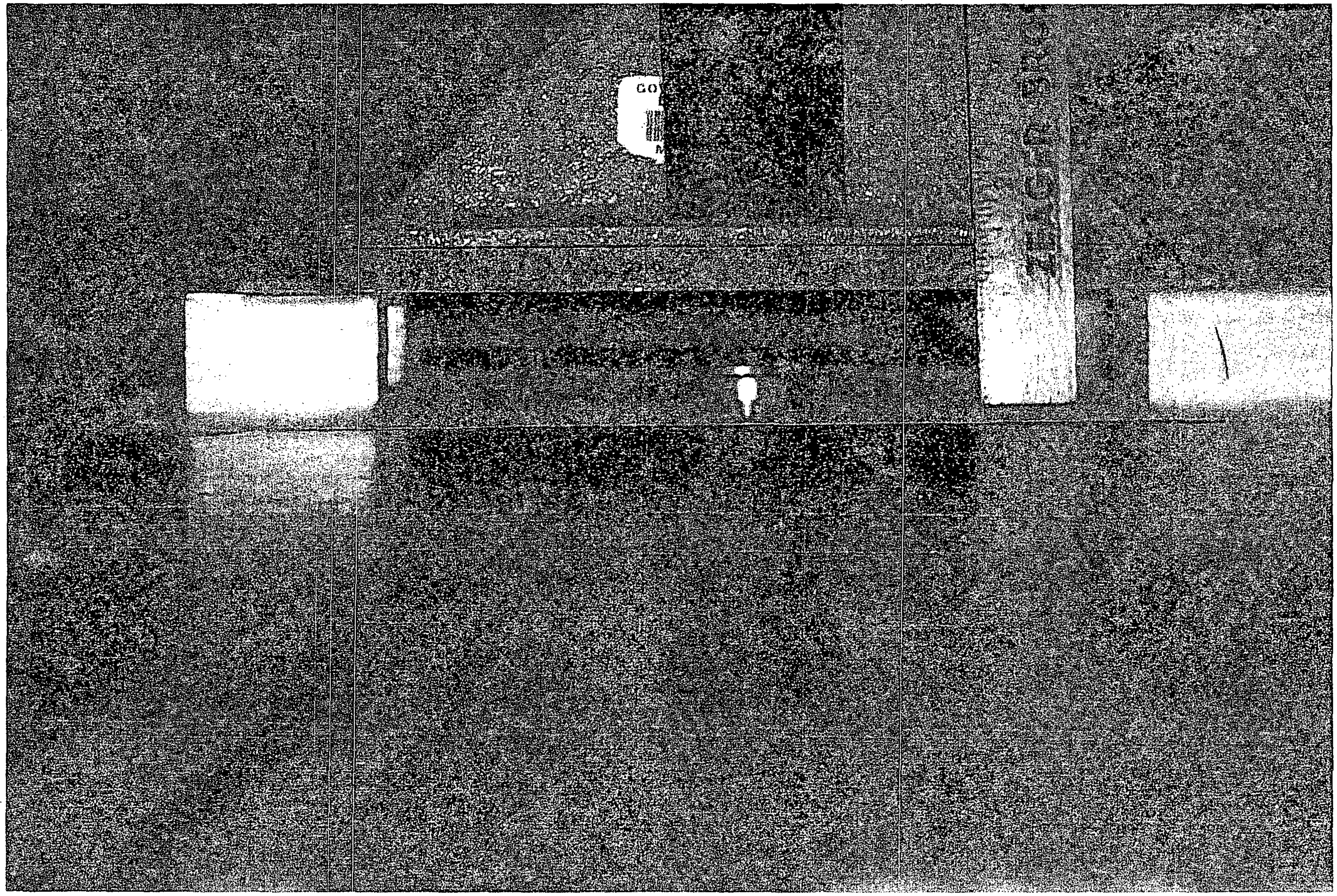

APPENDIX B

Data Obtained from a Ludlum Model 44-116 Plastic Scintillation Probe

(2 pages)

Summary of Data Collected Tuesday 12/18/07

background

No.	mean	mean+2σ	mean-2σ
1	152.1	170.197	134.003
2	155.9	180.799	131.001
3	148.4	179.828	116.972
4	143.8	186.745	100.855

avg of 3 sets of 10 one-minute counts

	mean	mean+2σ	mean-2σ
	149.367	183.633	115.100

avg of 4 sets of 10 one-minute counts

	mean	mean+2σ	mean-2σ
	150.05	180.944	119.156

0.010" aluminum shields

No.	mg/cm^2	mean	mean+2σ	mean-2σ
0	5.153	6475.8	6694.363	6257.238
1	73.702	2918.0	3014.203	2821.797
2	142.251	1942.2	2019.739	1864.661
3	210.800	1371.6	1443.093	1300.107
4	279.349	990.9	1045.830	935.970
5	347.897	705.2	764.348	646.052
6	416.446	519.2	569.672	468.728
7	484.995	388.8	433.080	344.520
8	553.544	298.3	333.828	262.772
9	622.093	234.8	259.091	210.509
10	690.641	202.0	239.947	164.053
11	759.190	183.4	215.026	151.774
12	827.739	166.8	188.542	145.058
13	896.288	161.3	185.995	136.605
14	964.837	159.2	179.129	139.271
15	1033.385	159.1	186.900	131.300
16	1101.934	160.2	183.097	137.303
17	1170.483	161.7	174.935	148.465
18	1239.032	159.0	182.017	135.983
19	1307.581	165.7	201.103	130.297
20	1376.129	157.5	191.221	123.779

range
areal density
density thickness

second check on 20 shields

No.	mg/cm^2	mean	mean+2σ	mean-2σ
20	1376.129	164.7	184.138	145.262

0.031207	air	0.010" air
68.58	aluminum	0.010" Al

acrylic/PVC combination

	mg/cm^2	mean	mean+2σ	mean-2σ
1/4"	interpolated from Al data **649**	221.3	245.687	196.913
1/2"	interpolated from Al data **827**	167.0	181.298	152.702
3/4"	calculated 1476	149.7	178.110	121.290

0.780179	air	0.255" air
589.407	PVC	0.255" PVC
calculated from 910 mg/cm^3 density		
1.52915	air	0.49" air
1132.586	PVC	0.49" PVC
calculated from 910 mg/cm^3 density		
2.309329	air	0.745" air
1721.993	PVC	0.745" PVC
calculated from 910 mg/cm^3 density		

stainless steel

	mg/cm^2	mean	mean+2σ	mean-2σ
thin	interpolated from Al data **445**	459.8	494.129	425.471
thick	interpolated from Al data **731**	190.8	215.018	166.582

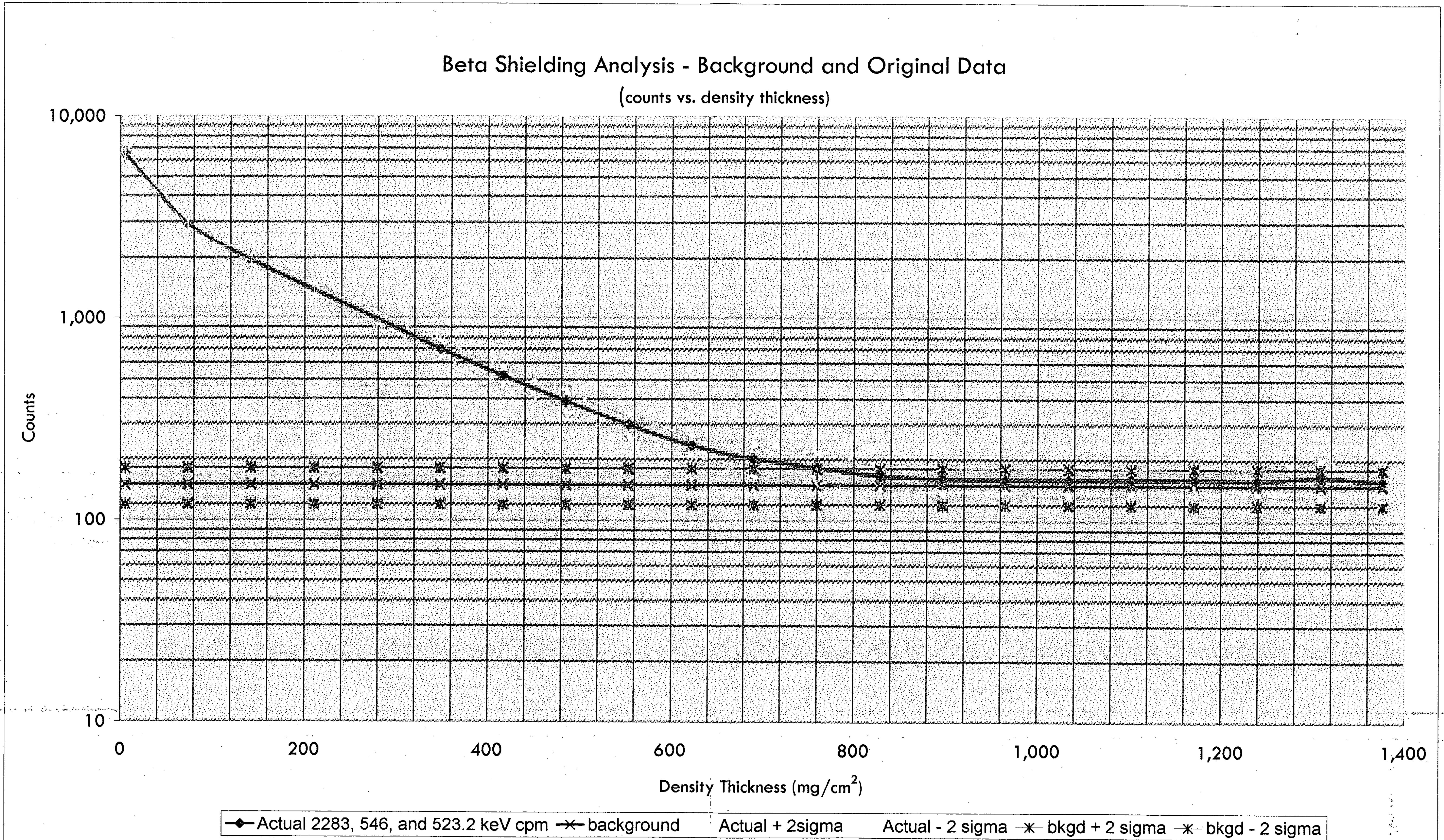
Beta Shielding Analysis - Background and Original Data
(counts vs. density thickness)
10,000
1,000
100
10
Counts
0
200
400
600
800
1,000
1,200
1,400
Density Thickness (mg/cm2)
Actual 2283, 546, and 523.2 keV cpm
background
Actual + 2sigma
Actual - 2 sigma
bkgd + 2 sigma
bkgd - 2 sigma

APPENDIX C

Derivations of Equations

(7 pages)

DERIVATIONS OF EQUATIONS

This appendix describes the derivations of equations used in this Technical Basis Document. The Least Squares Regression is used to estimate the actual activity due to Y-90 beta particle emission.

1.0 Introduction

A section of data in Appendix B, from 5.153 mg/cm^2 to 210.8 mg/cm^2 contains counts from the 0.546 MeV, 0.5232 MeV, and 2.2839 MeV beta particles. An attempt is being made to distinguish between the lower energy and higher energy betas to show how the activity of the 0.546 MeV and 0.5232 MeV betas fall off rather dramatically using very few aluminum sheets. The 2.2839 MeV beta particles are stopped by many sheets of aluminum.

Using data from 210.8 mg/cm^2 to 553.544 mg/cm^2, because it appears linear, an attempt will be made to estimate, by the method of least squares, the 2.2839 MeV beta counts back to 5.153 mg/cm^2. Though the data are plotted on semi-logarithmic paper, the equations derived are linear in form. Later, a transformation is used whereby the linear equations can be used to predict logarithmic y-axis values for each corresponding linear x-axis value. These logarithmic y-axis values will be subtracted from each corresponding total count to estimate the counts due to the 2.2839 MeV betas.

Values will be derived using the linear equation of the form $y = a + bx$. After the derivation, a transformation will be made to the linear equation to account for the fact that the data really fit an equation of the form $y = e^{(a + bx)}$ or $\ln y = a + bx$.

2.0 Theory

The theory behind the least squares regression is that the unknown parameters are estimated by minimizing the sum of the squared deviations between the actual data and the model (curve fit). By parameters is meant the lead coefficients in each term in the regression equation: the “a” and “b” values. The minimization process reduces the system of equations formed by the data to $\mathcal{P}$ equations (where $\mathcal{P}$ is the number of parameters in the functional part of the model) in $\mathcal{P}$ unknowns. This new system of equations is then solved to obtain the parameter estimates.

As with all statistical models, the method of least squares works within certain confines. The plusses and minuses of linear least square regression are listed below. The advantages of least squares are that:

A. Though there are types of data that are better described by functions that are non-linear in the parameters, many processes in science and engineering are well-described by linear models. This is because either the processes are inherently linear or because, over short ranges, any process can be well-approximated by a linear model.

B. Practically speaking, linear least squares regression makes very efficient use of the data. Good results can be obtained with relatively small data sets.

The disadvantages of least squares are that:

A. The main disadvantages of linear least squares are limitations in the shapes that linear models can assume over long ranges, possibly poor extrapolation properties, and sensitivity to outliers.

B. Linear models with non-linear terms in the predictor variables curve relatively slowly, so for inherently nonlinear processes it becomes increasingly difficult to find a linear model that fits the data well as the range of the data increases. As the explanatory variables become extreme, the output of the linear model will also be more extreme. This means that linear models may not be effective for extrapolating the results of a process for which data cannot be collected in the region of interest. Of course extrapolation is potentially dangerous regardless of the model type.

C. Finally, while the method of least squares often gives optimal estimates of the unknown parameters, it is very sensitive to the presence of unusual data points in the data used to fit a model. One or two outliers can sometimes seriously skew the results of a least squares analysis. This makes model validation, especially with respect to outliers, critical to obtaining sound answers to the questions motivating the construction of the model.

Fortunately, the data being analyzed cover a rather small range and, as mentioned in the opening paragraph of this section, appear linear.

3.0 Development of Equations

The equations are rather simple, but require a hint of calculus and a lot of algebra to understand. Derivations of the equations used in the method of least squares are shown below.

Generally, a curve fitting routine would start with an equation $y = a + bx + cx^2 + dx^3 + ...$ But, since our data look linear, only the first two terms apply and the equation becomes $y = a + bx$.

As mentioned previously, we want to minimize the sum of the squared deviations between the actual data and the model. Now we want to find the values of "a" and "b" which will achieve the minimum. Stating this mathematically

$G(a,b) = \sum_{i=1}^{n} [y_i - (a - bx_i)]^2$ where G(a,b) is just a function of the two variables "a" and "b" and "i" is just a counter from the first value to the sixth value since there are six sets of data used to derive this equation. Now, here is the hint of calculus. To find the minimum, we take the partial derivatives of our function with respect to "a" and "b" and set them equal to zero.

$$\frac{\partial G(a,b)}{\partial a} = -2\sum_{i=1}^{n}\left[y_i - (a - bx_i)\right] = 0 \quad \text{or} \quad \sum_{i=1}^{n}\left[y_i - (a - bx_i)\right] = 0 \qquad (1)$$

$$\frac{\partial G(a,b)}{\partial b} = -2\sum_{i=1}^{n}x_i\left[y_i - (a - bx_i)\right] = 0 \quad \text{or} \quad \sum_{i=1}^{n}x_i\left[y_i - (a - bx_i)\right] = 0 \qquad (2)$$

The rest is algebra. Expanding the equations above yields

$$\sum_{i=1}^{n} y_i - an - b\sum_{i=1}^{n} x_i = 0 \quad \text{or} \quad \sum_{i=1}^{n} y_i = an + b\sum_{i=1}^{n} x_i \qquad (3)$$

$$\sum_{i=1}^{n} x_i y_i - a\sum_{i=1}^{n} x_i - b\sum_{i=1}^{n} x_i^2 = 0 \quad \text{or} \quad \sum_{i=1}^{n} x_i y_i = a\sum_{i=1}^{n} x_i + b\sum_{i=1}^{n} x_i^2 \qquad (4)$$

Now we solve the two equations with two unknowns, "a" and "b".

Solving equation (3) for "a", we have $a = \dfrac{\sum_{i=1}^{n} y_i - b\sum_{i=1}^{n} x_i}{n}$ (5)

Substituting equation (5) into equation (4) yields

$$\sum_{i=1}^{n} x_i y_i = \left[\frac{\sum_{i=1}^{n} y_i - b\sum_{i=1}^{n} x_i}{n}\right]\sum_{i=1}^{n} x_i + b\sum_{i=1}^{n} x_i^2 \qquad (6)$$

Take equation (6) and multiply through by "n" to clear out the fractions

$$n\sum_{i=1}^{n} x_i y_i = \sum_{i=1}^{n} y_i \sum_{i=1}^{n} x_i - b\left[\sum_{i=1}^{n} x_i\right]^2 + nb\sum_{i=1}^{n} x_i^2 \qquad (7)$$

Now take the "b" terms in equation (7) and group them together

$$n\sum_{i=1}^{n} x_i y_i = \sum_{i=1}^{n} y_i \sum_{i=1}^{n} x_i + b\left[n\sum_{i=1}^{n} x_i^2 - \left(\sum_{i=1}^{n} x_i\right)^2\right] \qquad (8)$$

Solve equation (8) for "b"

$$b = \frac{n\sum_{i=1}^{n} x_i y_i - \sum_{i=1}^{n} y_i \sum_{i=1}^{n} x_i}{n\sum_{i=1}^{n} x_i^2 - \left(\sum_{i=1}^{n} x_i\right)^2} \qquad (9)$$

Now that "b" has been defined, we need to solve for "a" so we substitute equation (9) into equation (3)

$$\sum_{i=1}^{n} y_i = an + \left[\frac{n\sum_{i=1}^{n} x_i y_i - \sum_{i=1}^{n} y_i \sum_{i=1}^{n} x_i}{n\sum_{i=1}^{n} x_i^2 - \left(\sum_{i=1}^{n} x_i\right)^2}\right] \sum_{i=1}^{n} x_i \qquad (10)$$

Take equation (10) and multiply through by $n\sum_{i=1}^{n} x_i^2 - \left(\sum_{i=1}^{n} x_i\right)^2$ to clear out the fractions

$$n\sum_{i=1}^{n} y_i \sum_{i=1}^{n} x_i^2 - \sum_{i=1}^{n} y_i \left(\sum_{i=1}^{n} x_i\right)^2 =$$

$$an^2 \sum_{i=1}^{n} x_i^2 - an\left(\sum_{i=1}^{n} x_i\right)^2 + n\sum_{i=1}^{n} x_i y_i \sum_{i=1}^{n} x_i - \sum_{i=1}^{n} y_i \left(\sum_{i=1}^{n} x_i\right)^2 \qquad (11)$$

Notice how the last term on each side of the equal sign are identical so they can be cancelled

$$n\sum_{i=1}^{n} y_i \sum_{i=1}^{n} x_i^2 = an^2 \sum_{i=1}^{n} x_i^2 - an\left(\sum_{i=1}^{n} x_i\right)^2 + n\sum_{i=1}^{n} x_i y_i \sum_{i=1}^{n} x_i \qquad (12)$$

Take equation (12) and divide through by "n"

$$\sum_{i=1}^{n} y_i \sum_{i=1}^{n} x_i^2 = an\sum_{i=1}^{n} x_i^2 - a\left(\sum_{i=1}^{n} x_i\right)^2 + \sum_{i=1}^{n} x_i y_i \sum_{i=1}^{n} x_i \qquad (13)$$

Now take the "a" terms in equation (13) and group them together

$$\sum_{i=1}^{n} y_i \sum_{i=1}^{n} x_i^2 = a\left[n\sum_{i=1}^{n} x_i^2 - \left(\sum_{i=1}^{n} x_i\right)^2\right] + \sum_{i=1}^{n} x_i y_i \sum_{i=1}^{n} x_i \qquad (14)$$

Solve equation (13) for "a"

$$a = \frac{\sum_{i=1}^{n} y_i \sum_{i=1}^{n} x_i^2 - \sum_{i=1}^{n} x_i y_i \sum_{i=1}^{n} x_i}{n\sum_{i=1}^{n} x_i^2 - \left(\sum_{i=1}^{n} x_i\right)^2} \qquad (15)$$

The two equations (9) and (15) have now been solved for "a" and "b". Go to Appendix D for computation of the values for "a" and "b" and see a graph of the actual data and that predicted by the least squares regression.

4.0 Coefficient of Correlation

Once the values of "a" and "b" are determined, the line is defined, and plots of the actual versus predicted data (from the regression line) can be drawn. At this point, though we have both the actual and predicted data sets, we need to determine how well the data are correlated. The coefficient of correlation does exactly that.

The coefficient of correlation is a measure of the degree of association between the independent and dependent variable. The correlation coefficient is usually denoted by "r" and measures both the degree and indicates the direction of a relationship. The correlation coefficient varies between -1 and 1 ($-1 \leq r \leq +1$). The closer the r is to either +1 or -1 the stronger the linear association between two variables. Perfect correlations, identified by either $r = 1$ or $r = -1$, occur only when all data points lie exactly on a straight line. The closer "r" is to zero, the weaker the linear association. In fact, no correlation exists when $r = 0$. This means there is a completely random, non-linear relationship between the two variables. For background, a coefficient of correlation greater than 0.8 is generally considered strong, whereas a correlation coefficient less than 0.5 is generally considered weak. For example, if $r = 0.922$, then $r^2 = 0.850$ and 85% of the total variation between actual and predicted data can be explained by the linear relationship between "x" and "y". The other 15% of the total variation in "y" remains unexplained.

The sign of "r" indicates the direction of the relationship between an independent and dependent variable. If "x" and "y" denote independent and dependent variables, respectively, then a relationship is said to be positive and $r > 0$ if "y" increases as "x" increases. On the other hand, if "y" decreases as "x" increase, then $r < 0$ and the relationship is said to be negative.

The computational form of the coefficient of correlation [JOHN 1964] is provided below.

$$r = \frac{n\sum_{i=1}^{n} x_i y_i - \sum_{i=1}^{n} y_i \sum_{i=1}^{n} x_i}{\sqrt{\left[n\sum_{i=1}^{n} x_i^2 - \left(\sum_{i=1}^{n} x_i\right)^2\right]\left[n\sum_{i=1}^{n} y_i^2 - \left(\sum_{i=1}^{n} y_i\right)^2\right]}}$$

In Appendix D, the coefficient of correlation will be calculated and it will be determined how well the data correlate.

5.0 Equation Transformations

As mentioned previously, a transformation of the linear equation is needed because the data are actually related semi-logarithmically. Below are the transformation equations for “a”, “b”, and “r”. As can be seen, they simply replace y values with the natural logarithm of y.

ln y = a + bx

$$a = \frac{\sum_{i=1}^{n} \ln y_i \sum_{i=1}^{n} x_i^2 - \sum_{i=1}^{n} x_i \ln y_i \sum_{i=1}^{n} x_i}{n\sum_{i=1}^{n} x_i^2 - \left(\sum_{i=1}^{n} x_i\right)^2}$$

$$b = \frac{n\sum_{i=1}^{n} x_i \ln y_i - \sum_{i=1}^{n} \ln y_i \sum_{i=1}^{n} x_i}{n\sum_{i=1}^{n} x_i^2 - \left(\sum_{i=1}^{n} x_i\right)^2}$$

$$r = \frac{n\sum_{i=1}^{n} x_i \ln y_i - \sum_{i=1}^{n} \ln y_i \sum_{i=1}^{n} x_i}{\sqrt{\left[n\sum_{i=1}^{n} x_i^2 - \left(\sum_{i=1}^{n} x_i\right)^2\right]\left[n\sum_{i=1}^{n} (\ln y_i)^2 - \left(\sum_{i=1}^{n} \ln y_i\right)^2\right]}}$$

APPENDIX D

Determination of Coefficients

(3 pages)

DETERMINE COEFFICIENTS

Determining the leading coefficients for the least squares regression fit is accomplished by building a spreadsheet to ascertain the various summation values and then plugging them into the equations for "a" and "b". After that, a new graph of the original data and the values predicted by the least squares analysis will be plotted.

The table below shows data taken from the linear portion of the plot in Appendix B.

TABLE D-1
Density Thickness and Gross Counts

Density Thickness (mg/cm^2)	Gross Counts (cpm)
210.800	1371.6
279.349	990.9
347.897	705.2
416.466	519.2
484.995	388.8
553.544	298.3

The equations for the leading coefficients, from Appendix C, are shown below. Remember that n = 6 for this case because there are six sets of data.

$$a = \frac{\sum_{i=1}^{n} \ln y_i \sum_{i=1}^{n} x_i^2 - \sum_{i=1}^{n} x_i \ln y_i \sum_{i=1}^{n} x_i}{n\sum_{i=1}^{n} x_i^2 - \left(\sum_{i=1}^{n} x_i\right)^2} \qquad b = \frac{n\sum_{i=1}^{n} x_i \ln y_i - \sum_{i=1}^{n} \ln y_i \sum_{i=1}^{n} x_i}{n\sum_{i=1}^{n} x_i^2 - \left(\sum_{i=1}^{n} x_i\right)^2}$$

Below is a table of the inputs to the equations for leading coefficients "a" and "b"

TABLE D-2
Inputs to Solve Equations for "a", "b" and "r"

i	x_i	y_i	$\ln(y_i)$	$x_i\ln(y_i)$	x_i^2	$[\ln(y_i)]^2$
1	210.800	1371.6	7.223733221	1522.7630	44436.6400	52.1823
2	279.349	990.9	6.898613621	1927.1208	78035.8638	47.5909
3	347.897	705.2	6.558481451	2281.6760	121032.3226	43.0137
4	416.466	519.2	6.252289165	2603.8659	173443.9292	39.0911
5	484.995	388.8	5.963065073	2892.0567	235220.1500	35.5581
6	553.544	298.3	5.698099692	3154.1489	306410.9599	32.4683
summation	2293.05	4274.0000	38.5943	14381.6313	958579.8655	249.9045

a = 8.143327766 b = -0.004476867

In order to determine how closely the data are correlated, the correlation coefficient needs to be calculated. From Appendix C, the equation is

$$r = \frac{n\sum_{i=1}^{n} x_i \ln y_i - \sum_{i=1}^{n} \ln y_i \sum_{i=1}^{n} x_i}{\sqrt{\left[n\sum_{i=1}^{n} x_i^2 - \left(\sum_{i=1}^{n} x_i\right)^2\right]\left[n\sum_{i=1}^{n} (\ln y_i)^2 - \left(\sum_{i=1}^{n} \ln y_i\right)^2\right]}}$$

r = -0.999019689 r^2 = 0.998040339

For this example, r = -0.99902 and r^2 = 0.99804. This is a very strong correlation and means that 99.804% of the total variation can be explained by the linear relationship between "x" and "y" while 0.196% of the total variation is unexplained.

Below is a table showing the actual data obtained from Appendix B and that predicted by the equations derived in Appendix C.

TABLE D-3
Actual and Predicted 2283.9 keV Counts and Percent Difference

Density Thickness (mg/cm^2)	Actual Gross Counts (cpm)	Natural Log of Counts	Natural Log predicted by a + bx	Inverse Log predicted by $y = e^{(a + bx)}$	% difference of Counts
210.800	1371.6	7.2237	7.1996	1338.9007	2.3840
279.349	990.9	6.8986	6.8927	985.0766	0.5877
347.897	705.2	6.5585	6.5858	724.7590	-2.7735
416.466	519.2	6.2523	6.2789	533.1831	-2.6932
484.995	388.8	5.9631	5.9721	392.3168	-0.9045
553.544	298.3	5.6981	5.6652	288.6413	3.2379
				average	-0.0269

FIGURE D.1
Actual and Predicted 2283.9 keV Counts versus Density Thickness from a Sr/Y-90 Source

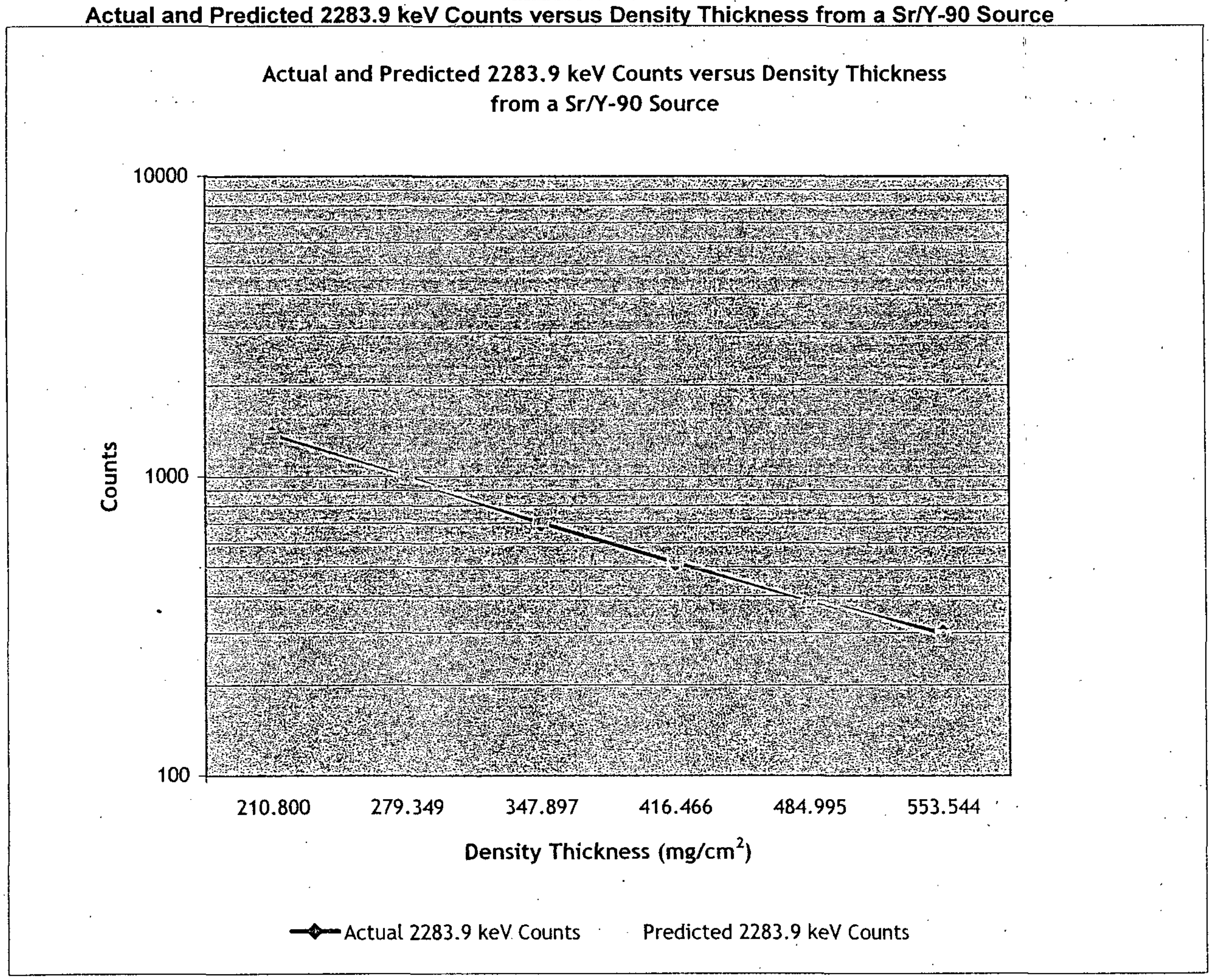

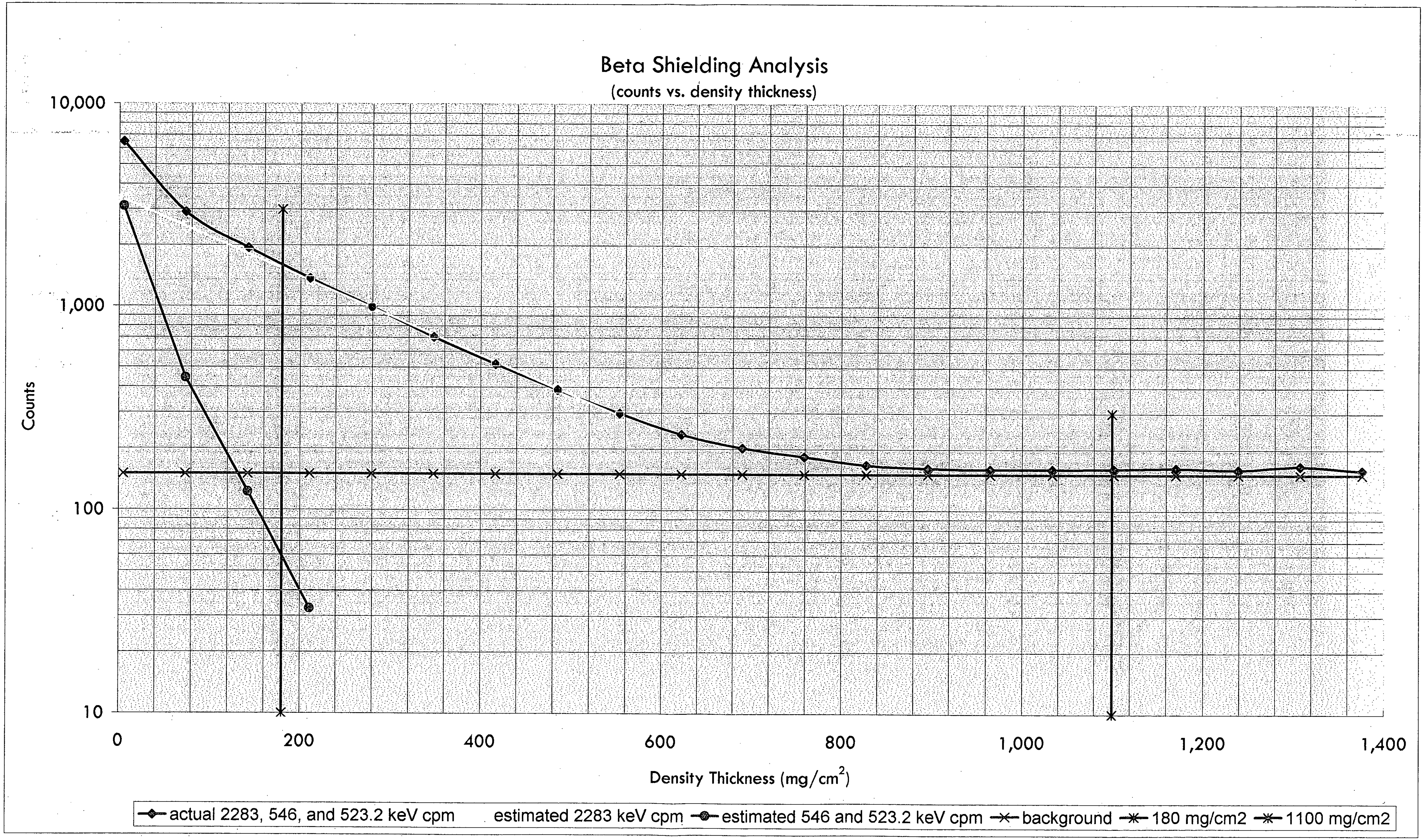
Beta Shielding Analysis
(counts vs. density thickness)
10,000
1,000
100
10
Counts
0
200
400
600
800
1,000
1,200
1,400
Density Thickness (mg/cm²)
actual 2283, 546, and 523.2 keV cpm
estimated 2283 keV cpm
estimated 546 and 523.2 keV cpm
background
180 mg/cm2
1100 mg/cm2